ResearchGate

See discussions, stats, and author profiles for this publication at: https://www.researchgate.net/publication/15436008

750 MHz 1H-C NMR spectroscopy of human blood plasma

ARTICLE *in* ANALYTICAL CHEMISTRY · APRIL 1995

Impact Factor: 5.64 · DOI: 10.1021/ac00101a004 · Source: PubMed

CITATIONS
660

READS
144

5 AUTHORS, INCLUDING:

Jeremy K Nicholson
Imperial College London
740 PUBLICATIONS **43,846** CITATIONS
SEE PROFILE

Manfred Spraul
Bruker BioSpin
175 PUBLICATIONS **7,325** CITATIONS
SEE PROFILE

Duncan Farrant
Cambridge Display Technology
80 PUBLICATIONS **2,963** CITATIONS
SEE PROFILE

Available from: Jeremy K Nicholson
Retrieved on: 29 January 2016

Anal. Chem. **1995**, *67*, 793–811

750 MHz ^{1}H and ^{1}H–^{13}C NMR Spectroscopy of Human Blood Plasma

Jeremy K. Nicholson* and Peta J. D. Foxall

Department of Chemistry, Birkbeck College, University of London, Gordon House, 29 Gordon Square, London WC1H 0PP, U.K.

Manfred Spraul

Bruker Analytische Messtechnik GmbH, D76287-Rheinstetten, Silberstreifen, Germany

R. Duncan Farrant and John C. Lindon

Department of Physical Sciences, Wellcome Research Laboratories, Beckenham, Kent BR3 3BS, U.K.

High-resolution 750 MHz ^{1}H NMR spectra of control human blood plasma have been measured and assigned by the concerted use of a range of spin–echo, two-dimensional *J*-resolved, and homonuclear and heteronuclear (^{1}H–^{13}C) correlation methods. The increased spectral dispersion and sensitivity at 750 MHz enable the assignment of numerous ^{1}H and ^{13}C resonances from many molecular species that cannot be detected at lower frequencies. This work presents the most comprehensive assignment of the ^{1}H NMR spectra of blood plasma yet achieved and includes the assignment of signals from 43 low M_r metabolites, including many with complex or strongly coupled spin systems. New assignments are also provided from the ^{1}H and ^{13}C NMR signals from several important macromolecular species in whole blood plasma, i.e., very-low-density, low-density, and high-density lipoproteins, albumin, and α_1-acid glycoprotein. The temperature dependence of the one-dimensional and spin–echo 750 MHz ^{1}H NMR spectra of plasma was investigated over the range 292–310 K. The ^{1}H NMR signals from the fatty acyl side chains of the lipoproteins increased substantially with temperature (hence also molecular mobility), with a disproportionate increase from lipids in low-density lipoprotein. Two-dimensional ^{1}H–^{13}C heteronuclear multiple quantum coherence spectroscopy at 292 and 310 K allowed both the direct detection of cholesterol and choline species bound in high-density lipoprotein and the assignment of their signals and confirmed the assignment of most of the lipoprotein resonances.

During the last decade, a diverse range of ^{1}H NMR spectroscopic studies has been performed on vertebrate biological fluids in relation to the investigation of toxicological processes, metabolic diseases, and drug metabolism.[1–5] Considerable effort has gone into obtaining useful biochemical information from ^{1}H NMR spectra of blood plasma. Early successful attempts in this area were focused on the measurement of mobile, low M_r metabolites in whole blood plasma using Hahn spin–echo (HSE) experiments to attenuate the broad signals from lipoproteins and other macromolecules which dominate the one-dimensional (1-D) spectra.[6] HSE experiments on blood plasma were found to be useful for the simultaneous investigation of ketone body (3-D-hydroxybutyrate, acetoacetate, and acetone) production, perturbed amino acid metabolism, and changes in mobile lipid levels in human subjects with diabetes mellitus and hypertriglyceridemias.[7] There have also been many more recent attempts to use ^{1}H NMR spectra of plasma to provide novel diagnostic information on metastatic tumors based on measurements of composite lipoprotein signal line widths.[8–12] This has led to numerous investigations into the limitations of this approach and to a detailed evaluation of both the causes of variation in the ^{1}H NMR signals of plasma lipoproteins and the computer fitting of complex line shapes which arise from the long-chain CH_2 and terminal CH_3 signals from the different lipoprotein components.[13–19] Although in principle these

(1) Nicholson, J. K.; Wilson, I. D. *Prog. Nucl. Magn. Reson. Spectrosc.* **1989**, *21*, 449–501.
(2) Nicholson, J. K., Wilson, I. D. In *Drug Metabolism–from Molecules to Man* Benford, D. J., Bridges, J. W., Gibson, G. G., Eds.; Taylor Francis: London, 1987; pp 189–207.
(3) Malet Martino, M. C.; Martino, R. *Biochemie* **1992**, *74*, 785–800.
(4) Holmes, E.; Foxall, P. J. D.; Nicholson, J. K. *J. Pharm. Biomed. Anal.* **1990**, *8*, 955–958.
(5) Foxall, P. J. D.; Mellotte, G.; Bending, M.; Lindon, J. C.; Nicholson, J. K. *Kidney Int.* **1993**, *43*, 234–245.
(6) Nicholson, J. K.; Buckingham, M. J.; Sadler, P. J. *Biochem. J.* **1983**, *211*, 605–615.
(7) Nicholson, J. K.; O'Flynn, M. P.; Sadler, P. J.; Macleod, A. F.; Juul, S. M.; Sonksen, P. H. *Biochem. J.* **1984**, *217*, 365–375.
(8) Fossel, E. T.; Carr, J. M.; McDonagh, J. *N. Engl. J. Med.* **1986**, *315*, 1369–1376.
(9) Mountford, C. E.; Tattersall, M. H. N. *Cancer Surveys* **1987**, *6*, 285–314.
(10) Bradamante, S.; Barchesi, E.; Pilotti, S.; Borasi, G. *Magn. Reson. Med.* **1988**, *8*, 440–449.
(11) Buchthal, S. D.; Hardy, M. A.; Brown, T. R. *Am. J. Med.* **1988**, *85*, 528–532.
(12) Fossel, E. T. *Cancer Cells* **1991**, *3*, 173–182.
(13) Bell, J. D.; Brown, J. C. L.; Norman, R. E.; Sadler, P. J.; Newell, D. R. *NMR Biomed.* **1988**, *1*, 90–94.
(14) Herring, F. G.; Phillips, P. S.; Pritchard, P. H. *J. Lipid Res.* **1989**, *30*, 521–528.
(15) Herring, F. G.; Phillips, P. S.; Pritchard, P. H.; Silver, H.; Whittal, K. P. *Magn. Reson. Med.* **1990**, *16*, 35–48.
(16) Otvos, J. D.; Jeyarajah, E. J.; Hayes, L. W.; Freedman, D. S.; Janjan, N. A.; Anderson, T. *Clin. Chem.* **1991**, *37*, 369–376.
(17) Otvos, J. D.; Jeyarajah, E. J.; Bennett, D. W. *Clin. Chem.* **1991**, *37*, 377–385.

0003-2700/95/0367-0793$9.00/0 © 1995 American Chemical Society

experiments can give useful clinical data on whole blood plasma, full exploitation of the potential of high-resolution NMR to give biochemical information is hampered by the incompleteness of the assignment data and a poor understanding of the dynamic intermolecular interactions that occur in blood plasma.

All biological fluids are highly complex mixtures of metabolites, and even 1-D high-frequency ^{1}H NMR spectra may contain many thousands of resolved NMR resonance lines with varying degrees of signal overlap, depending on the fluid type and the chemical shift range under consideration.[6,20] As with all high-resolution NMR experiments, the exact observation frequency at which the measurements are performed influences signal dispersion, sensitivity, and the relaxation properties of the nuclei in molecules under study. Given the complexity of the biofluid matrix, the frequency at which ^{1}H NMR spectra are measured has a major effect on the amount of chemical and biochemical information that can be obtained. Most biological fluids are effectively isotropic solutions and are much more magnetically homogeneous than, e.g., whole body, organ, tissue, or even cell preparations. This should make the interpretation of high-resolution NMR data more reliable and hence should lead to the discovery of new biochemical information. However, despite the powerful armory of multipulse and multidimensional NMR tools available, the complexity of the spectra and the degree of signal overlap have hindered the comprehensive assignment of the ^{1}H NMR spectra of most biofluids. Certain biofluids have been partially characterized by the use of 600 MHz ^{1}H NMR measurements, with many resonance assignments for the low M_r components of blood plasma,[20] cerebrospinal fluid,[21] and seminal fluid.[22] The recent development of 750 MHz ^{1}H NMR spectroscopy, with its significant improvement in spectral dispersion and sensitivity, provides the possibility to extend further the knowledge of the composition of biological fluids and the dynamic interaction of their component metabolites and macromolecular species. As many of the molecules of interest are small in size, they have short rotational correlation times and hence relatively long ^{1}H relaxation times. For heteronuclei, there is little chance of experiencing detrimental line-broadening effects of chemical shift anisotropy relaxation, which may occur, for example, in ^{13}C NMR spectra of ^{13}C-labeled macromolecules measured at such high frequencies. Unlike the ^{1}H NMR spectra of single substances (within the molecular mobility range of effective NMR observation), the total assignment of blood plasma spectra must always be incomplete because each sample is unique and subject to individual biological variation. However, the detailed assignment of the ^{1}H NMR spectra of plasma is necessary in order to obtain precise bioanalytical and dynamic information from the whole fluid and ultimately to enable greater precision in diagnoses in clinical and toxicological investigations. 750 MHz ^{1}H NMR spectroscopy clearly offers the best means so far for completing the signal assignment of whole blood plasma.

Blood plasma is a complex multicompartmental or multiphasic system with many different types of simultaneously occurring intermolecular interactions, including metal complexation and chemical exchange reactions, micellar compartmentation of metabolites, enzyme-mediated biotransformations, and the binding of small molecules by macromolecules.[1] ^{1}H NMR measurements made at very high observation frequencies should confer a number of benefits, because along with the sensitivity and dispersion factors, there is also a reduction in the number of observed second-order coupling effects and a change in the time scale of NMR-monitored events which may be particularly important for the observation of chemically exchanging species. In a preliminary study, we reported the use of standard one-dimensional, spin–echo, and two-dimensional *J*-resolved 600 and 750 MHz ^{1}H NMR spectroscopy of blood plasma to extend the known assignments of metabolite signals in the plasma of a normal individual, compared the metabolite profile with that of a patient with chronic renal failure, and indicated some of the advantages of 750 MHz measurements.[23] In the present study, we have comprehensively assigned the spectra of normal blood plasma using a range of one- and two-dimensional 750 MHz ^{1}H NMR and ^{1}H–^{13}C NMR techniques together with different data processing methods and investigated the effects of temperature change on the 750 MHz ^{1}H NMR spectra of human plasma.

MATERIALS AND METHODS

Blood from seven adult male volunteers was collected by venipuncture into lithium heparinized vacutainers, and the plasma was separated by centrifugation, snap-frozen, and stored at −40 °C prior to NMR measurement. Each subject had fasted overnight, and the blood was collected in the morning preprandially. The samples were thawed immediately before use, and 0.7 mL of each was diluted by 10% with D_2O to provide a field-frequency lock. ^{1}H chemical shifts were referenced internally to the α-glucose H_1 resonance at δ 5.233, measured relative to the primary internal chemical shift reference trimethylsilyl [2,2,3,3-$^2H_4$]propionate at δ 0.00. ^{1}H NMR spectra were measured on otherwise untreated biofluid samples at 750.14 MHz on a Bruker AMX 750 spectrometer at ambient probe temperature (292 K), and selected samples were also remeasured at 298, 304, and 310 K. As the temperature readings on standard NMR spectrometer variable temperature control units may be subject to calibration errors, the exact internal temperature of the samples (T_{plasma}) was measured from the chemical shift difference[24] between the ^{1}H NMR signal of H_2O and the H_1 signal of α-glucose using the following equation:

$$T_{plasma} = 84.17\Delta_\alpha + 17.23\Delta_\alpha^2 + 256.87$$

where $\Delta_\alpha = \delta(H_1,\alpha\text{-glucose}) - \delta(H_2O)$. Selected plasma samples were also measured on a Bruker ARX 400 spectrometer operating at 400.13 MHz using a 5 mm inverse geometry broadband probe.

In order to suppress the large water signal, all 1-D 750 MHz ^{1}H NMR spectra were acquired using a pulse sequence based on the two-dimensional NOE experiment[25] called NOESYPRESAT, comprising the following pulse sequence:

$$RD-90°-t_1-90°-t_m-90°-\text{acquire FID}$$

where RD is a relaxation delay of 1–3 s, during which the water

(18) Hiltunen, Y.; Ala-Korpela, M.; Jokisaari, J.; Eskelinen, S.; Kiviniitty, Y. A. *Magn. Reson. Med.* **1992**, *26*, 89–99.
(19) Ala-Korpela, M.; Heitvenen, Y.; Jokisaari, J.; Eskelinen, S.; Kiviniitty, K.; Savolainen, M. J.; Kesaniemi, Y. A. *NMR Biomed.* **1993**, *6*, 225–233.
(20) Foxall, P. J. D.; Parkinson, J.; Sadler, I. H.; Lindon, J. C.; Nicholson, J. K. *J. Pharm. Biomed. Anal.* **1993**, *11*, 21–31.
(21) Sweatman, B.; Farrant, R. D.; Holmes, E.; Ghauri, F. Y. K.; Lindon, J. C.; Nicholson, J. K. *J. Pharm. Biomed. Anal.* **1993**, *11*, 651–664.
(22) Lynch, M.; Masters, J.; Prior, J.; Spraul, M.; Foxall, P. J. D.; Lindon, J. C.; Nicholson, J. K. *J. Pharm. Biomed. Anal.* **1994**, *12* (1), 5–19.
(23) Foxall, P. J. D.; Spraul, M.; Farrant, R. D.; Lindon, J. C.; Neild, G. H.; Nicholson, J. K. *J. Pharm. Biomed. Anal.* **1993**, *11*, 267–276.

resonance is selectively irradiated; t_1 represents the first increment in a NOESY experiment and is set to 3 μs; and t_m, the mixing time in the NOESY sequence, has a value of 100–150 ms, during which the water resonance was again selectively irradiated. Typically 128 transients were collected into 64*K* data points with a spectral width of 10 000 Hz. The NOESYPRESAT pulse sequence results in attenuation factors of 10^5 or more for water signals in biofluid samples, thus eliminating the potentially severe dynamic range problem. For samples measured at lower frequencies, spectral widths were reduced and pulse recycle times adjusted to maintain the digital resolution and the relaxation delays equal to those for the 750 MHz measurements. Prior to Fourier transform (FT), exponential line-broadenings of 0.2–0.5 Hz were applied to the FIDs, which were also zero-filled by a factor of 2. Resolution enhancement of spectra was obtained through the application of the Lorentzian–Gaussian transformation method. Selected 1-D spectra were also analyzed using the maximum entropy method incorporated into Bruker UXNMR software (Memsys 5, Maxent Solutions Ltd., Cambridge, U.K.).

Carr–Purcell–Meiboom–Gill (CPMG) spin–echo spectra[26] were measured on all seven samples and the FIDs collected into 64*K* data points with a total spin–spin relaxation delay ($2n\tau$) of 87.8 ms and a total delay between pulse cycles of 4.28 s. For two of the plasma samples measured at 750 MHz, standard 1-D and CPMG spectra were remeasured at 292 K under comparable chemical shift range and relaxation conditions on a Bruker ARX 400 at 400.13 MHz, again with solvent presaturation. Variable temperature experiments were performed on two control plasma samples, which were measured successively using consecutive standard 1-D and CPMG experiments at 292, 298, 304, and 310 K and then remeasured at 292 K.

Two-dimensional *J*-resolved (JRES) spectra[27] were measured with solvent presaturation on each plasma sample at 292 or 304 K. The transients were collected into 8192 data points with a spectral width of 8064 Hz, and the F1 (*J*-coupling) domain spectral width covered 63 Hz with 64 increments of t_1 and eight transients were collected for each t_1 increment. Prior to the double FT and magnitude calculation, the F1 data were zero-filled to 1024 computer points and apodized by means of a sine-bell function in t_2 and a sine-bell-squared function in t_1. The spectra were tilted by 45° to provide orthogonality of the chemical shift and coupling constant axes and subsequently symmetrized about the F1 axis. Spectra were displayed both in the form of contour plots and as skyline F2 projections.

750 MHz ^{1}H–^{1}H correlation[28] spectroscopy (COSY-45 version) was performed on three plasma samples with water presaturation. Transients were acquired into 4096 data points with 16 scans per increment, a spectral width of 10 000 Hz, and 512 increments in the F1 axis, which was zero-filled to 2048 prior to FT. The relaxation delay between successive pulse cycles was 2.7 s. The data sets were weighted using a sine-bell function in t_1 and t_2 prior to FT. 750 MHz ^{1}H–^{1}H total correlation spectroscopy (TOCSY[29]) was performed on two samples to confirm the ^{1}H NMR assignments, particularly on lipids with chains of coupled protons. The spectra were collected in the phase-sensitive mode using time-proportional phase incrementation (TPPI), and the MLEV17 pulse sequence was used for the spin-lock.[30] The spectral width was 10 000 Hz, with data collected into 4096 time domain points. Typically 512 increments were measured with 16 transients per increment, the data set being zero-filled to 1024 in t_1, and a sine-bell-squared apodization function was applied prior to FT.

750 MHz ^{1}H–^{13}C phase-sensitive (TPPI) heteronuclear multiple quantum correlation (HMQC) spectra[31] were collected for two of the plasma samples with ^{1}H detection using an inverse geometry triple nucleus probe at both 292 and 310 K. A relaxation delay of 2.1 s was used between pulses, and a refocussing delay equal to $1/2^1J_{C-H}$ (3.57 ms) was employed. Composite pulse broadband ^{13}C decoupling (globally alternating optimized rectangular pulses, GARP) was used during the acquisition period.[32] Typically 2048 data points with 64 scans per increment and 400 experiments were acquired with spectral widths of 8064 Hz in F2 and 27.7 kHz in F1. The FIDs were weighted using a shifted sine-bell-squared function in F2 and exponential line-broadening of 0.3 Hz with forward complex linear prediction[33] to 800 data points in F1 prior to FT and two-dimensional phasing. To aid signal assignments for blood plasma, a series of 1-D ^{1}H NMR and ^{1}H–^{13}C HMQC spectra were measured at 310 K on a Bruker AMX 600 spectrometer operating at 600.13 MHz on the following substances (all from Sigma U.K.): human serum albumin (HSA, 40 g/L), low-density lipoprotein (LDL, 5 g/L), high-density lipoprotein (HDL, 10 g/L), human α_1-acid glycoprotein (100 g/L), and cholesterol linoleate (2 g/L), all made up in H_2O/D_2O (10:1), except for cholesteryl linoleate, where a 1:2:1 mixture of CD_3OD/D_2O/DMSO-d_6 was used. Two-dimensional ^{1}H–^{13}C HMQC data sets were enhanced using the technique of forward linear prediction on the real data points to twice the number of time domain points in the ^{13}C dimension.

RESULTS AND DISCUSSION

Assignment of One- and Two-Dimensional 750 MHz ^{1}H and ^{1}H–^{13}C NMR Spectra of Blood Plasma. Through the increased spectral dispersion of 750 MHz measurements and via the employment of appropriate 2-D NMR methods, we have been able to extend considerably the assignment of resonances in blood plasma spectra in normal individuals undergoing a standard overnight fast. Assignments are based on comparison of chemical shifts and spin–spin coupling constants with those of model compounds measured in phosphate buffer at pH 7.4, with the signals detected in the various 1- and 2-D experiments performed on plasma. In general, resonances have not been assigned unless all of the ^{1}H NMR signals for a given molecule were resolved. In addition, proof of spin–spin coupling connectivity within a given molecule was obtained via the use of 2-D correlation spectroscopy (see below). In summary, a comprehensive list of the 43 ^{1}H NMR-detectable low M_r metabolites and the assigned macromolecular signals observed in human plasma, together with their spin systems and their ^{1}H chemical shifts (and ^{13}C shifts where available), is given in Table 1. A detailed consideration of the contributions of each of the major NMR experiments used in the

(24) Farrant, R. D.; Nicholson, J. K.; Lindon, J. C. *NMR Biomed.* **1994**, *7*, 243–247.
(25) Jeener, J.; Meier, B. H.; Bachmann, P.; Ernst, R. R. *J. Chem. Phys.* **1979**, *71*, 4546–4553.
(26) Meiboom, S.; Gill, D. *Rev. Sci. Instrum.* **1958**, *29*, 688–691.
(27) Aue, W. P.; Karham, J.; Ernst, R. R. *J. Chem. Phys.* **1976**, *64*, 4226–4227.
(28) Nagayama, K.; Kumar, A.; Wuthrich, K.; Ernst, R. R. *J. Magn. Reson.* **1980**, *40*, 321–334.
(29) Bax, A.; Davis, D. G. *J. Magn. Reson.* **1985**, *65*, 355–360.
(30) Bax, A.; Subramanian, S. *J. Magn. Reson.* **1986**, *67*, 565–569.
(31) Bax, A.; Griffey, R. H.; Hawkins, B. L. *J. Magn. Reson.* **1983**, *55*, 301–315.
(32) Shaka, A. J.; Barker, P. B.; Freeman, R. *J. Magn. Reson.* **1985**, *64*, 547–552.
(33) Stephenson, D. S. *Prog. Nucl. Magn. Reson. Spectrosc.* **1988**, *20*, 515–626.

Table 1. Resonance Assignments with Chemical Shifts and Spin–Spin Coupling Patterns of Metabolites Identified in 750 MHz ^{1}H and ^{1}H–^{13}C NMR Spectra of Normal Human Blood Plasma[a]

^{1}H shift (δ)	multiplicity	molecule	assignment	observed	^{13}C shift (δ)
0.66	m	cholesterol	C18 (in HDL)	1D, HMQC	12.6
0.70	m	cholesterol	C18 (in VLDL)	HMQC	
0.84	m	cholesterol	C26 and C27	HMQC	23.3
0.84	t	lipid (mainly LDL)	$CH_3(CH_2)_n$	1D, JRES, COSY, HMQC	14.7
0.87	t	lipid (mainly VLDL)	$CH_3CH_2CH_2C$=	1D, JRES, COSY	
0.91		cholesterol	C21	HMQC	19.4
0.93	m	lipid	CH_3CH_2	COSY	
0.93	t	isoleucine	δ-CH_3	1D, JRES, COSY	
0.95	d	leucine	δ-CH_3	1D, JRES, COSY	
0.97	d	leucine	δ-CH_3	1D, JRES, COSY	
0.97	d	valine	CH_3	1D, JRES, COSY, HMQC	19.6
1.00	d	isoleucine	β-CH_3	1D, JRES, COSY, HMQC	14.6
1.02	d	valine	CH_3	1D, JRES, COSY	
1.13	d	isobutyrate	CH_3	CPMG, JRES	
1.20	d	3-hydroxybutyrate	γ-CH_3	1D, CPMG, JRES	
1.22	m	lipid	$CH_3CH_2CH_2$	HMQC	32.7
1.25	m	lipid (mainly LDL)	$(CH_2)_n$	1D, CPMG, JRES, COSY, HMQC	30.6
1.26	m	lipid	$CH_3CH_2(CH_2)_n$	COSY, HMQC	23.2
1.28	m	isoleucine	half γ-CH_2	COSY	
1.29	m	lipid (mainly VLDL)	$CH_2CH_2CH_2CO$	1D, CPMG, JRES, COSY	
1.30	m	lipid	CH_2	COSY, HMQC	19.7
1.31	d	fucose	CH_3	CPMG, JRES, COSY	
1.32	d	threonine	γ-CH_3	JRES, COSY	
1.32	m	lipid	$CH_2CH_2CH_2CO$	COSY	
1.33	d	lactate	CH_3	JRES, COSY, HMQC	20.9
1.46	d	alanine	CH_3	1D, CPMG, JRES, COSY, HMQC	16.8
1.47	m	isoleucine	half γ-CH_2	JRES, COSY	
1.48	m	lysine	γ-CH_2	CPMG, COSY, HMQC	
1.57	m	lipid (mainly VLDL)	CH_2CH_2CO	JRES, COSY, HMQC	25.6
1.57	m	citrulline	γ-CH_2	ID, COSY	
1.68	m	arginine	γ-CH_2	ID, CPMG, COSY	
1.69	m	lysine	δ-CH_2	1D, COSY	
1.69	m	lipid	CH_2CH_2C=C	1D, JRES, HMQC	27.4
1.71	m	leucine	β-CH_2, γ-CH	COSY, HMQC	40.7
1.86	m	citrulline	β-CH_2	COSY	
1.91	m	lysine	β-CH_2	JRES, COSY, HMQC	30.3
1.91	m	arginine	β-CH_2	COSY	
1.91	s	acetate	CH_3	JRES, CPMG	
1.96	m	isoleucine	β-CH	COSY	
1.97	m	lipid	CH_2C=C	1D, COSY	
1.99	m	proline	γ-CH_2	COSY	
2.00	m	lipid	CH_2C=C	COSY, HMQC	27.8
2.00	m	lipid	CH_2C=C	COSY	
2.00	m	glutamate	half β-CH_2	JRES, COSY	
~2.04	s	glycoprotein[b] (acetyls)	$NHCOCH_3$	1D, JRES, HMQC	23.0
2.05	m	proline	half β-CH_2	COSY	
2.08	m	glutamine	half β-CH_2	1D, JRES, COSY	
2.09	m	glutamine	half β-CH_2	1D, JRES, COSY	
2.13	s	methionine	S-CH_3	CPMG, JRES	
2.14	m	glutamate	half β-CH_2	1D, JRES, COSY, HMQC	30.1
2.22	s	acetoacetate	CH_3	CPMG, JRES	
2.23	m	lipid	CH_2CO	COSY, HMQC	34.6
2.24	spt of d	valine	β-CH	COSY	
2.31	m	3-hydroxybutyrate	half α-CH_2	CPMG, JRES, COSY	
2.36	m	glutamate	half γ-CH_2	COSY, HMQC	34.5
2.36	s	pyruvate	CH_2	ID, CPMG, JRES, CPMG	
2.36	m	proline	half β-CH_2	COSY	
2.38	m	3-hydroxybutyrate	half α-CH2	JRES, COSY	
2.39	ABX	U1[c]	CH_2	COSY	
2.41	m	glutamine	half γ-CH_2	CPMG, JRES, COSY, HMQC	31.9
2.47	t	2-oxoglutarate	γ-CH_2	JRES	
2.52	d	citrate	half CH_2	JRES, COSY	
2.54	s	methylamine	CH_3	CPMG, JRES	
2.54	ABX	U1[c]	CH_2	COSY	
2.68	dd	aspartate	half β-CH_2	JRES	
2.69	d	citrate	half CH_2	JRES, COSY	
2.69	m	lipid	C=CCH_2C=C	COSY	
2.71	s	dimethylamine	CH_3	CPMG, JRES	
2.71	m	lipid	C=CCH_2C=C	1D, COSY	
2.72	m	lipid	C=CCH_2C=C	1D, COSY, HMQC	26.2
2.81	dd	aspartate	half β-CH_2	JRES	
2.83	s	trimethylamine	CH_3	1D, CPMG, JRES	
2.84	dd	asparagine	half β-CH_2	JRES	
2.89	t	albumin lysyl	ϵ-CH_2	1D, COSY, HMQC	40.3
2.94	dd	asparagine	half β-CH_2	JRES	

Table 1 (Continued)

^{1}H shift (δ)	multiplicity	molecule	assignment	observed	^{13}C shift (δ)
2.96	t	albumin lysyl	ϵ-CH_2	1D, COSY, HMQC	40.3
3.01	t	albumin lysyl[d]	ϵ-CH_2	1D, JRES, COSY, HMQC	40.3
3.04	s	creatine	CH_3	CPMG, JRES	
3.05	s	creatinine	CH_3	1D, CPMG, JRES	
3.06	dd	tyrosine	half β-CH_2	JRES, COSY	
3.12	dd	phenylalanine	half β-CH_2	JRES	
3.14	dd	histidine	half β-CH_2	JRES	
3.15	t	citrulline	γ-CH_2	JRES	
3.16	dd	tyrosine	half β-CH_2	JRES, COSY	
3.21	s	choline	$N(CH_3)_3$	JRES, HMQC	55.0
3.24	t	arginine	δ-CH_2	COSY, HMQC	41.3
3.24	dd	β-glucose	H2	1D, JRES, COSY, HMQC	75.1
3.25	dd	histidine	half β-CH2	JRES	
3.25	t	taurine	CH_2NH	JRES	
3.26	s	TMAO	CH_3	JRES	
3.26	t	U2[c]	ABX	COSY	
3.26	dd	phenylalanine	half β-CH_2	COSY	
3.28	t	*myo*-inositol	H5	JRES	
3.34	m	proline	half δ-CH_2	COSY	
3.40	t	β-glucose	H4	1D, JRES, COSY, HMQC	70.6
3.41	t	taurine	CH_2SO_3	JRES	
3.42	t	α-glucose	H4	JRES, COSY, HMQC	70.6
3.45	m	proline	half δ-CH_2	COSY	
3.47	ddd	β-glucose	H5	JRES, COSY, HMQC	76.7
3.48	dd	threonine	α-CH	JRES, COSY	
3.48	t	β-glucose	H3	JRES, COSY, HMQC	76.7
3.54	dd	α-glucose	H2	JRES, COSY, HMQC	72.3
3.54	dd	U2[c]	CH	COSY, HMQC	
3.54	s	glycine	CH_2	CPMG, JRES	
3.56	dd	*myo*-inositol	H1, H3	JRES	
3.56	dd	glycerol	half CH_2	1D, JRES, COSY	63.5
3.57	d	valine	α-CH	JRES, COSY, HMQC	64.2
3.60	d	threonine	α-CH	JRES	
3.63	dd	*myo*-inositol	H4, H6	JRES	
3.64	dd	glycerol	half CH_2	1D, JRES, COSY	63.5
3.66	m	choline (lipid)	NCH_2	COSY, HMQC	66.7
3.68	t	glutamine	α-CH_2	JRES, COSY, HMQC	55.4
3.69	dd	leucine	α-CH	JRES, COSY, HMQC	55.1
3.70	m	citrulline	α-CH	COSY	
3.71	t	α-glucose	H3	JRES, COSY, HMQC	73.6
3.72	dd	α-glucose	half CH_2-C6	JRES, COSY, HMQC	61.6
3.75	m	U1[c]	α-CH	COSY	
3.76	m	α-glucose	half CH_2-C6	JRES, COSY, HMQC	61.4
3.76	q	alanine	α-CH	JRES, COSY	
3.83	ddd	α-glucose	H5	JRES, COSY, HMQC	72.3
3.84	m	α-glucose	half CH_2-C6	JRES, COSY, HMQC	61.4
3.87	m	glycerol	C2-H	JRES, COSY	72.6
3.90	dd	β-glucose	half CH_2-C6	JRES, COSY, HMQC	61.6
3.93	s	creatine	CH_2	JRES	
3.94	dd	tyrosine	α-CH	JRES	
3.97		phenylalanine	α-CH	JRES, COSY	
3.98	dd	histidine	α-CH	JRES	
3.98	ABX	U2[c]	CH	COSY, HMQC	
4.05	s	creatinine	CH_2	1D, JRES	
4.06	m	glyceryl of lipids	CH_2OCOR	HMQC	62.5
4.06	t	*myo*-inositol	H2	JRES	
4.11	q	lactate	CH	1D, JRES, COSY, HMQC	69.2
4.12	m	proline	α-CH	JRES, COSY	
4.13	m	3-hydroxybutyrate	β-CH	1D, JRES, COSY	
4.24	m	threonine	β-CH	1D, JRES, COSY	
4.25	m	glyceryl of lipids	CH_2OCOR	HMQC	62.5
4.29	m	choline (lipid)	OCH_2	HMQC	60.2
4.53	d	β-galactose	H1	JRES	
4.64	d	β-glucose	H1	1D, CPMG, JRES, COSY, HMQC	
5.20	m	glyceryl of lipids	CHOCOR	COSY	
5.23	d	α-glucose	H1	1D, CPMG, JRES, COSY, HMQC	92.9
5.23	m	unsaturated lipid	$CH{=}C\mathit{H}CH_2C\mathit{H}{=}CH$	1D, COSY	128.6
5.26	m	unsaturated lipid	$CH{=}C\mathit{H}CH_2C\mathit{H}{=}CH$	1D, COSY, HMQC	128.6
5.27	m	unsaturated lipid	$=C\mathit{H}CH_2CH_2$	1D, COSY	
5.29	m	unsaturated lipid	$CH{=}C\mathit{H}CH_2C\mathit{H}{=}CH$	1D, COSY	128.6
5.31	m	unsaturated lipid	$=C\mathit{H}CH_2CH_2$	1D, COSY, HMQC	130.1
5.33	m	unsaturated lipid	$=C\mathit{H}CH_2CH_2$	1D, COSY	
6.87	m	tyrosine	H3, H5	1D, CPMG, HMQC	116.7
7.01	s	3-methylhistidine	H4	1D, CPMG, JRES	
7.02	s	histidine	H4	ID, CPMG, JRES	
7.05	s	1-methylhistidine	H4	ID, CPMG, JRES	

Table 1 (Continued)

^{1}H shift (δ)	multiplicity	molecule	assignment	observed	^{13}C shift (δ)
7.17	m	tyrosine	H2, H6	CPMG, JRES, COSY	
7.33	m	phenylalanine	H2, H6	1D, CPMG, COSY	
7.38	m	phenylalanine	H4	1D, CPMG, COSY	
7.43	m	phenylalanine	H3, H5	1D, CPMG, COSY	
7.61	s	3-methylhistidine	H2	1D, CPMG, JRES	
7.73	s	histidine	H2	ID, CPMG	
7.77	s	1-methylhistidine	H2	CPMG, JRES	
8.45	s	formate	CH	1D, CPMG	

[a] Abbreviations and Key: s, singlet; d, doublet; t, triplet; q, quartet; spt, septet; m, complex multiplet; dd, doublet of doublets; ddd, doublet of doublets of doublets. Chemical shifts all referenced to H-1 and C-1 of α-glucose at 5.233 for ^{1}H and at 92.9 ppm for ^{13}C. [b] Mainly α_1-acid glycoprotein. [c] U1 and U2 refer to unidentified metabolites. [d] Indicates overlap of free lysine with albumin lysyl and α_1-acid glycoprotein signals.

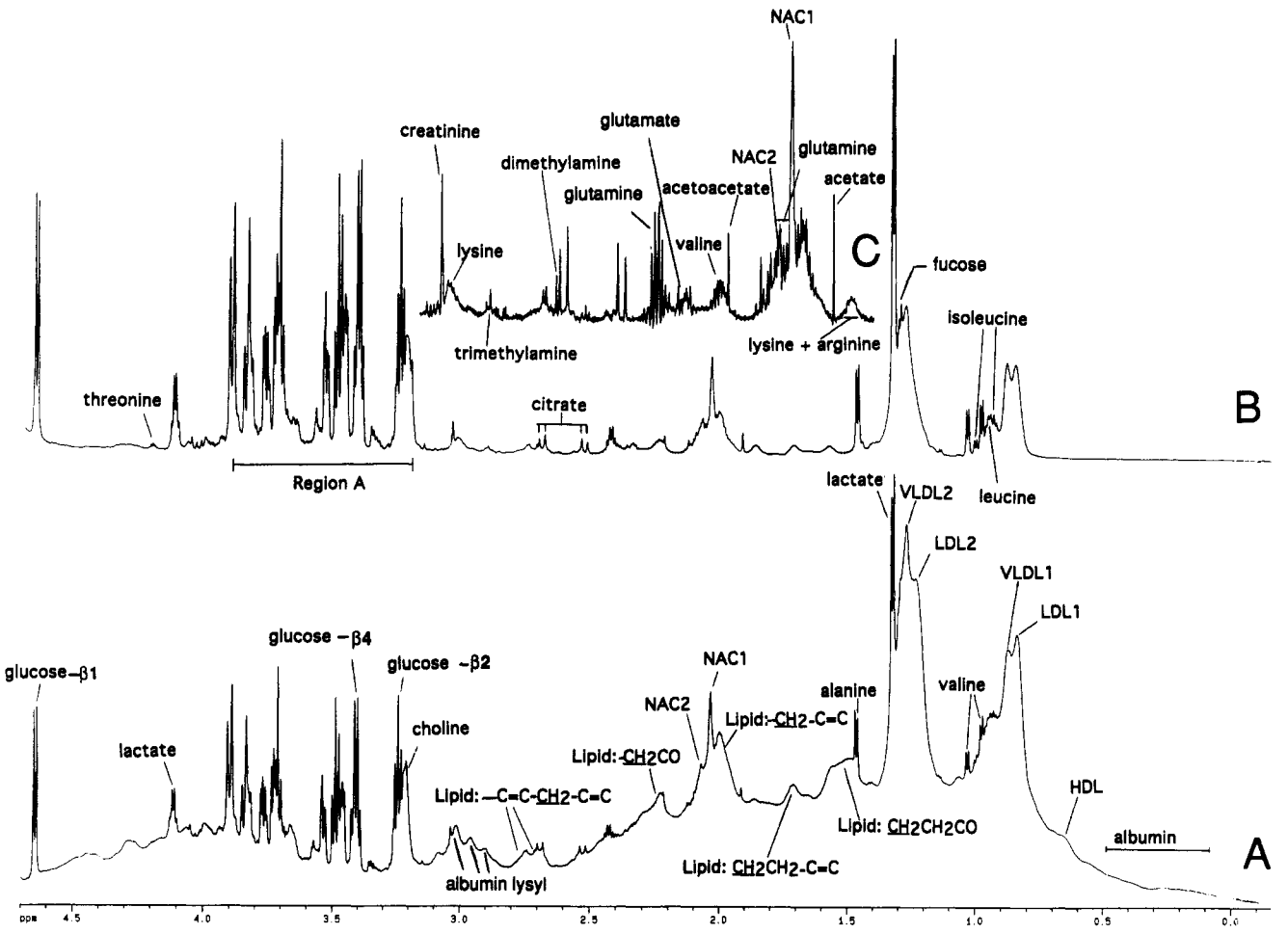

Figure 1. 750 MHz ^{1}H NMR spectra (δ −0.2 to 4.7) of control human blood plasma measured at 292 K: (A) 1-D spectrum, (B) CPMG spin−echo spectrum, and (C) expansion of resolution-enhanced CPMG spin−echo spectrum (δ 1.8−3.1). Abbreviations: LDL1 and VLDL1 refer to the terminal CH_3 groups of fatty acids in low-density and very-low-density lipoproteins, respectively; HDL refers to the C18 signal from cholesterol in high-density lipoprotein; NAC1 and NAC2 refer to composite acetyl signals from α_1-acid glycoprotein. The region in spectrum A labeled "albumin" indicates the position of poorly resolved signals from ring current-shifted protons from amino acids in albumin. Other assignments are as labeled. The area labeled "Region A" in spectrum B contains signals from glycerol, glucose, and amino acid CH protons.

signal assignment process is given below, together with descriptions of the influence of temperature and the frequency dependence of the spectra.

One-Dimensional ^{1}H NMR Spectroscopy of Blood Plasma. Standard 1-D ^{1}H NMR spectra of human blood plasma are very complex, and resonances of low M_r metabolites, proteins, lipids, and lipoproteins are heavily overlapped, even at 750 MHz, but nonetheless, many resonances can be assigned (Figure 1A). These include the terminal CH_3, various types of CH_2 groups from the long-chain fatty acids present in lipoproteins, and the $N^+(CH_3)_3$ groups of choline-containing molecules in lipoproteins. Strong signals from the ϵ-CH_2 protons in at least three magnetically distinct lysyl groups from albumin in regions of high molecular mobility can also be observed (not previously assigned in whole blood plasma), together with the *N*-acetyl groups of acetylated amino sugar moieties on highly mobile regions of α_1-acid glycoprotein.[34-36] Signals from a large number of small molecular species can also be observed superimposed upon the broader

(34) Bell, J. D.; Brown, J. C. C.; Nicholson, J. K.; Sadler, P. J. *FEBS Lett.* **1987**, *215*, 311−315.

resonances from the macromolecules (Figure 1A). At 750 MHz, the AB spin system of citrate is resolved for the first time in standard 1-D spectra of blood plasma.

The complex ^{1}H NMR profile of blood plasma can be simplified by use of spin–echo experiments with appropriate T_2 relaxation delays to attenuate signals from broad macromolecular components and other protein-bound compounds.[6,7] The effect of applying the CPMG spin–echo pulse sequence to blood plasma at 750 MHz is shown in Figure 1B, and a partial expansion with Lorentzian–Gaussian resolution enhancement is shown in Figure 1C. A substantial reduction in the contribution from protein and lipoprotein signals is achieved with the use of a short total spin–spin relaxation delay ($2n\tau$ = 88 ms), and, unlike the HSE sequence, all the peaks are in phase. HSE techniques have been used previously to help assign spectra of blood plasma and have been successfully applied in clinical studies on perturbed metabolite profiles associated with various organic disease processes.[6,7] The list of low M_r metabolites detected in earlier 400 or 500 MHz HSE ^{1}H NMR studies of untreated blood plasma was limited to acetate, acetoacetate, acetone, alanine, choline, creatinine, creatine, formate, glucose, glutamine, glycerol, histidine, 3-D-hydroxybutyrate, isoleucine, lactate, threonine, tyrosine, and valine.[1,6,7,37] Earlier assignments were, in general, based on the observation of only one or two resonances for each metabolite. In 750 MHz CPMG spectra, it is also possible to detect arginine, dimethylamine, lysine, and trimethylamine and to resolve many of the glucose resonances from both α- and β-anomers. The CH_3 resonance of fucose can also be detected although having a chemical shift between the lactate signal and the composite lipoprotein CH_2 signals; this has only previously been reported in plasma or plasma extracts in 2-D experiments performed at lower frequency.[9]

In previous 400 and 500 MHz NMR studies of blood plasma, two CH_3 signals from the acetylated glycan moieties present in regions of high molecular mobility of certain glycoproteins including α_1-acid glycoprotein have been observed with use of spin–echo experiments (using $2n\tau$ values of 120–136 ms), and these signals have been partially assigned and used diagnostically.[6,7,34–36] Resolution-enhanced 750 MHz CPMG spectra ($2n\tau$ = 88 ms) of human blood plasma (Figure 1C) show many more resolved lines in the region from δ 1.9 to 2.1; some of these arise from low M_r species such as glutamate and glutamine, but many others probably also arise from glycoproteins. The *N*-acetyl signal centered at δ 2.04 is also partially overlapped with the broad $CH_2C{=}C$ signals from several plasma lipoproteins, which are not resolved at 400 MHz (see below and Table 1). The expansion of a typical 750 MHz ^{1}H CPMG spectrum of a blood plasma sample is shown in Figure 2A, with no postacquisition data processing other than FT. With Lorentzian–Gaussian resolution enhancement prior to FT (Figure 2B), at least 35 lines can be resolved in the composite set of peaks from δ 1.93 to 2.15 (see Figure 3 for further assignment). The use of maximum entropy signal processing reveals even greater underlying complexity, with >60 resolved lines in the same region of the spectrum, but still showing evidence of extensive peak overlap. Evidence of the validity of the maximum entropy result is provided in Figure 2, which shows

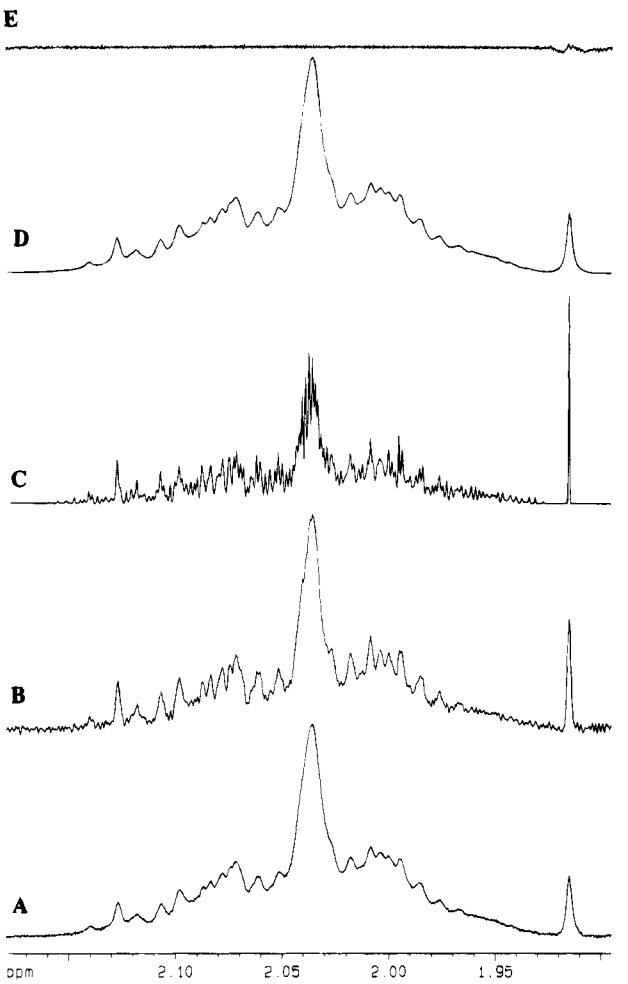

Figure 2. Resolution-enhanced and maximum entropy-processed 750 MHz ^{1}H CPMG spin–echo NMR spectrum (656 scans) of a control human blood plasma sample measured at 292 K (δ 1.89–2.18), including the region depicting the *N*-acetyl resonances of glycoprotein moieties. (A) Raw data with no FID weighting, baseline corrected to remove broad components; (B) Lorentzian–Gaussian resolution-enhanced spectrum (parameters, LB = −3, GB = 0.22); (C) Memsys 5 quantified maximum entropy result with a Lorentzian point spread function at full width at half-height of 2.30 Hz (based on value for acetate at δ 1.92); (D) mock data, i.e., the result shown in spectrum C convolved with the point spread function; and (E) difference spectrum produced by the subtraction of spectrum D from spectrum A.

the reconstructed or "mock" data obtained by convolution of the maximum entropy solution with the line point spread function (Figure 2D) and the near perfect computer subtraction (Figure 2E) of the mock data from the real data as shown in Figure 2A. Particularly dramatic is the effect of maximum entropy processing on the large and apparently broad peak centered at δ 2.03, observed in the unprocessed data and assigned to an α_1-acid glycoprotein moiety.[34–36] The complex underlying structure in the peak is due to the proximity of at least six singlets from *N*-acetyl groups of sialic acid residues in slightly different chemical environments, probably representing contributions from the acetylated glycan species at different branching points on oligosaccharide chains at the α_1-acid glycoprotein surface as previously suggested.[34] Clearly, further work is needed at a very high NMR frequency in order to provide more detailed assignment information on these glycoprotein-related signals. The relationships between NMR observation frequency and the information

(35) Kriat, M.; Confort-Gouny, S.; Vion-Drury, J.; Viout, P.; Cozzone, P. J. *Biochemie* **1992**, *74*, 913–918.
(36) Grootveld, M.; Claxson, A. W. D.; Chander, C. L.; Haycock, P.; Blake, D. R.; Hawkes, G. E. *FEBS Lett.* **1993**, *322* (3), 266–276.
(37) Nicholson, J. K.; Gartland, K. P. R. *NMR Biomed.* **1989**, *2*, 63–70.

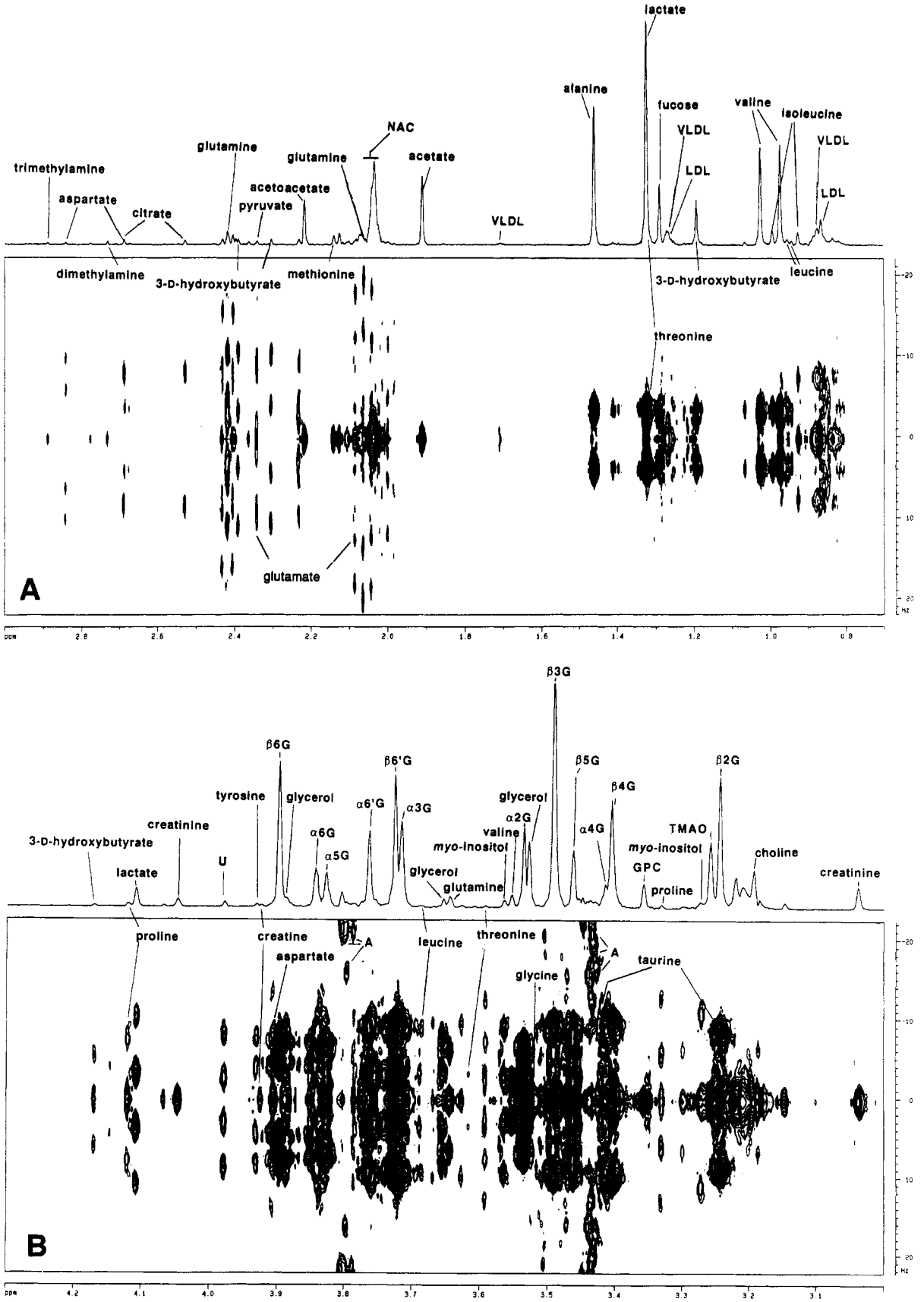

Figure 3. 750 MHz ^{1}H JRES NMR spectrum of a control human blood plasma sample measured at 292 K with skyline F2 projections. (A) Spectral region covering δ 0.7–3.0 and (B) spectral region covering the range δ 3.0–4.3. Assignments are as labeled; LDL and VLDL signals are as assigned in Figure 1 and Table 1. NAC indicates the residual composite signal of acetyl signals from α_1-acid glycoprotein; TMAO indicates trimethylamine *N*-oxide; U indicates an unidentified metabolite signal; and A indicates strong coupling artifacts. The peaks labeled α1G–α6G and β1G–β6G indicate the appropriate signals from α- and β-glucose, respectively.

content of biofluid spectra are discussed later; however, it is important to note that the quantitative measurement of the α_1-acid glycoprotein and possibly other glycoprotein-related ^{1}H NMR peaks in plasma to aid disease diagnosis, as advocated by other workers,[35,36] must be treated with caution because of the problems of peak overlap at lower frequencies and the lack of detailed assignment data.

The signals from some lipid and lipoprotein components, e.g., very-low-density lipoprotein (VLDL), LDL, HDL, and chylomicrons, have also been partially characterized, but assignment has been limited by the use of lower frequency spectrometers, the extensive chemical shift overlap, and the broadness of the signals due to the short proton T_2 relaxation times of these large supramolecular species.[6,7,13,17] In the 1-D spectrum of blood plasma in the chemical shift region from δ 0.7 to 1.5, there is a variety of overlapping signals from small organic species such as lactate, 3-D-hydroxybutyrate, alanine, and branched chain amino acids, together with the terminal CH_3 and long-chain $(CH_2)_n$ groups of fatty acid-containing moieties integral to the various lipoprotein particles, especially VLDL, LDL, and HDL. The line widths of the composite signals centered at approximately δ 1.2 and 0.8 have been measured at lower frequencies in a number of previous studies, and it has been suggested that the arithmetic mean of the line width of the two composite signals may in some way relate to the presence of metastatic tumors in the donor.[8] This work has been extensively investigated elsewhere,[13-19] and the subject remains highly controversial because of the composite nature of the peaks, which may severely limit the reliability of any test based on simple line width measurements. The lipid and lipoprotein line widths are also subject to many other extraneous influences, including temperature, sample preparation, and spectrometer frequencies, and these are discussed in greater detail below. The 750 MHz spectra in Figure 1 show that the signals from LDL, VLDL, and HDL can be more clearly resolved in whole plasma than has previously been possible, [9,13] suggesting that very-high-frequency NMR measurements will be necessary to further the understanding of the variability of plasma lipoprotein composition and molecular mobility in relation to disease processes.

Two-Dimensional *J*-Resolved Spectroscopy of Blood Plasma. We have previously shown the value of making JRES measurements on biofluids at 600 and 750 MHz to aid spectral assignment of blood plasma and other biofluids.[20,21,23] The aliphatic region of the 750 MHz ^{1}H JRES spectrum of a typical plasma sample is shown in Figure 3 and has been plotted in two separate subsections for display purposes. The JRES spectrum, being based on a spin−echo pulse sequence, gives weak signals from substances with short ^{1}H T_2 values, such as macromolecules, motionally constrained low M_r species, and species involved in chemical exchange processes occurring at intermediate rates on the NMR time scale. Contributions from such broad signals are suppressed further by the use of sine-bell-squared functions in the JRES data processing. Consequently, the signals from LDL and VLDL that dominate the 1-D spectra and are still strong in CPMG spin−echo spectra are virtually eliminated from the JRES spectra, except for the vestigial peaks from the terminal CH_3 and chain CH_2 protons.

It is well known that second-order NMR spin systems give rise to artifact peaks in JRES spectra; however, the NMR spectra of the small endogenous molecules are in general first order at 750 MHz, and these give relatively simple JRES contour patterns (Figure 3). Metabolites that give second-order spectra even at 750 MHz include glucose, glutamine, and glutamate. The strongly coupled protons give rise to artifacts in the JRES spectra at the average δ values of the coupled spin systems (labeled A in Figure 3). Most of the assigned metabolite peaks are labeled in the JRES spectrum shown in Figure 3, and other peaks have also been assigned, although the scaling used for optimal display of the spectra precludes identification in the figure. All of the resonances assigned in the JRES and the other 2-D spectra are given in Table 1. The region of the JRES spectrum to high frequency of the water signal contains only signals from formate, histidine, and tyrosine (seen only in three of the seven individuals studied, data not shown). Taurine gives rise to two CH_2 triplets, and these have now been assigned in plasma for the first time (only seen in the contour plots), as has the AX spin system of aspartate and the α-CH resonances of valine and alanine (not shown in Figure 3). A doublet is observed at δ 1.31 which is assigned to fucose, and this was confirmed by a COSY connectivity to the C5-H proton of fucose at δ 4.28.[9] However, further COSY coupling connectivities are not seen due to the known small (ca. 1 Hz) C5-H to C4-H spin−spin coupling in fucose.[38] Fucose has previously been identified only in the NMR spectra of plasma of cancer patients.[9]

Methylamine, dimethylamine, trimethylamine, and trimethylamine *N*-oxide give sharp singlets for their *N*-CH_3 groups, and all of these substances give signals that are disproportionately strong in JRES skyline projections (relative to others observed in 1-D experiments) because of their relatively long ^{1}H T_2 relaxation times. The choline $N^+(CH_3)_3$ group gives a broader signal at δ 3.21, which is mainly from the choline present in HDL[39] but may also have contributions from choline in phospholipids from other lipoproteins. For 3-D-hydroxybutyrate, all ^{1}H signals can be observed (in those plasma samples containing this metabolite), and these consist of both halves of the nonequivalent CH_2, the CHOH, and the CH_3 resonances. Singlets from pyruvate, succinate, and acetate were assigned on the basis of chemical shifts of standard compounds. Isobutyric acid was also detected in some samples for the first time, giving a CH_3 doublet at δ 1.13 (not shown). The JRES spectrum is also useful for resolving the resonances in the δ 2.0−2.15 region, which include those of the highly mobile *N*-acetyl groups of glycoproteins. Clearly there is one major peak from *N*-acetyl groups and from several other glycoprotein-related singlets in this region. In addition, multiplets from the nonequivalent β-CH_2 protons of glutamate and glutamine are also present, which are partially responsible for the complexity of the maximum entropy processed 1-D spectra in this region, as shown in Figure 2. The AB spin system of citrate is also clearly visible in the JRES spectra of most plasma samples, although these can be difficult to observe in single pulse spectra because of peak overlap. The resonances from many amino acids are clearly observed, but certain others expected to be present in NMR-detectable quantities, e.g., phenylalanine,[40] were not detected because they are significantly broadened by binding to macromolecular components.[37] However, weak signals from tyrosine and histidine were observed in JRES spectra from three of the subjects, indicating the presence of a motionally unconstrained fraction of these metabolites. The variability of the JRES spectra from control individuals appears to be quite small, as seen from the stacked plot of the JRES projections of the plasma from five other subjects (Figure 4). The stacked plot provides a "^{1}H decoupled" ^{1}H spectrum and also provides a simple and useful

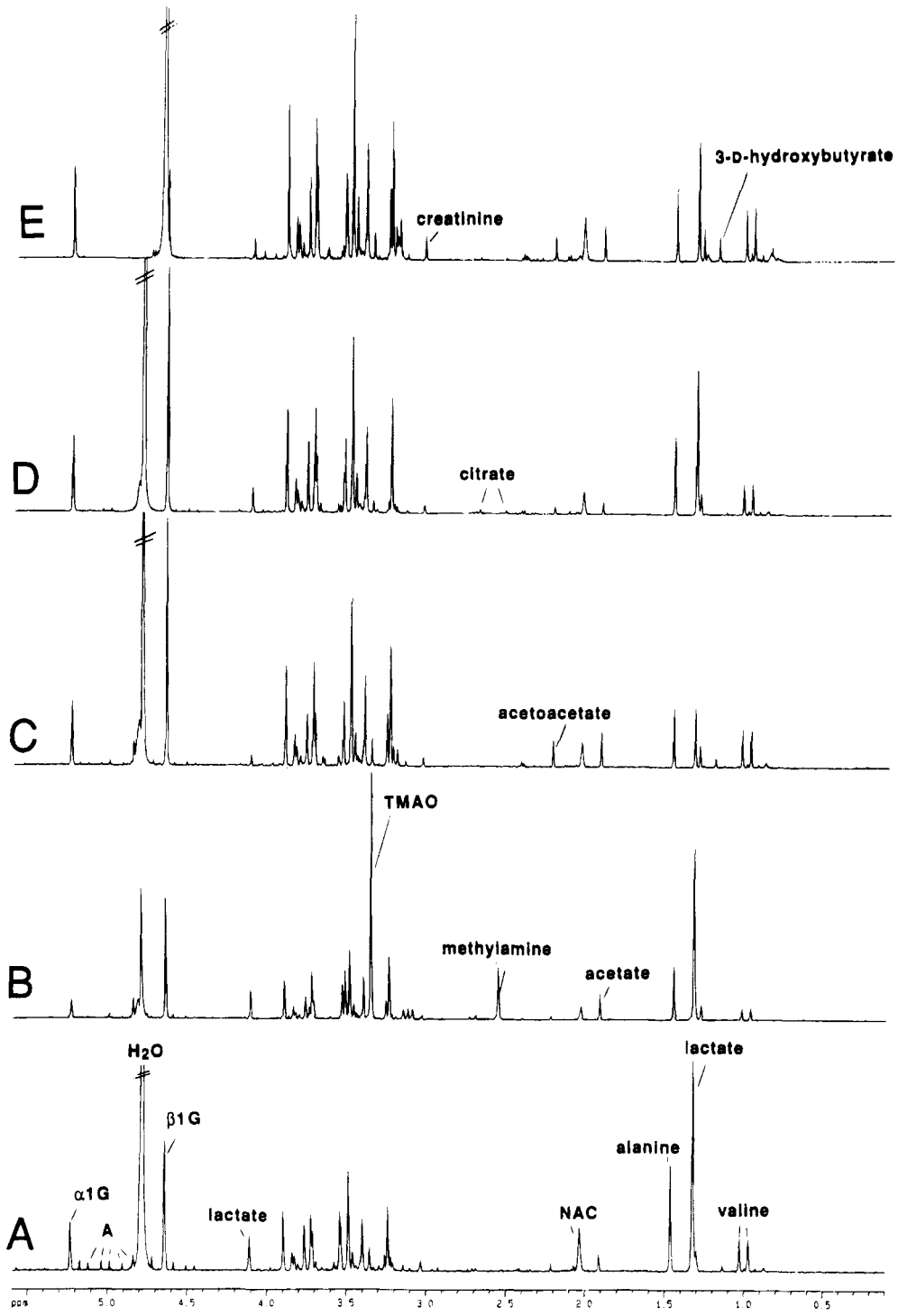

Figure 4. Skyline projections of the 750 MHz ^{1}H JRES NMR spectra from the blood plasma of five control subjects: (A)−(D) measured at 292 K and (E) measured at 304 K. Assignments are as labeled. Others are given in Table 1. Abbreviations are as used in Figure 3.

method for comparing a series of complex JRES spectra of biofluids. The most variable metabolites detected in JRES spectra appear to be lactate, acetate, methylamine, citrate, and TMAO, which are most likely concerned with variations in diet and recency of eating or exercise. Variation in temperature would also lead to significant artifactual changes in the residual lipoprotein signal intensities in JRES spectra, as increased temperatures increase the molecular mobility (see below).

Two-Dimensional ^{1}H−^{1}H Correlation Spectroscopy of Blood Plasma. A 750 MHz ^{1}H−^{1}H COSY-45 spectrum of plasma processed using forward linear prediction to improve resolution is shown in Figure 5. Many of the regions of the COSY spectrum require significant vertical expansion to visualize the less intense or more complex cross-peaks. This figure depicts a magnitude presentation spectrum, but improved resolution for some peaks has been obtained from phase-sensitive COSY and TOCSY experiments (not shown). The 750 MHz ^{1}H−^{1}H COSY spectra show strong connectivities for protons from low M_r metabolites and for the major macromolecular lipoprotein components. COSY spectra of blood plasma give information that is complementary to the JRES spectra, but interactive 2-D assignment is partly limited by the differences in the molecular motion ranges of the plasma

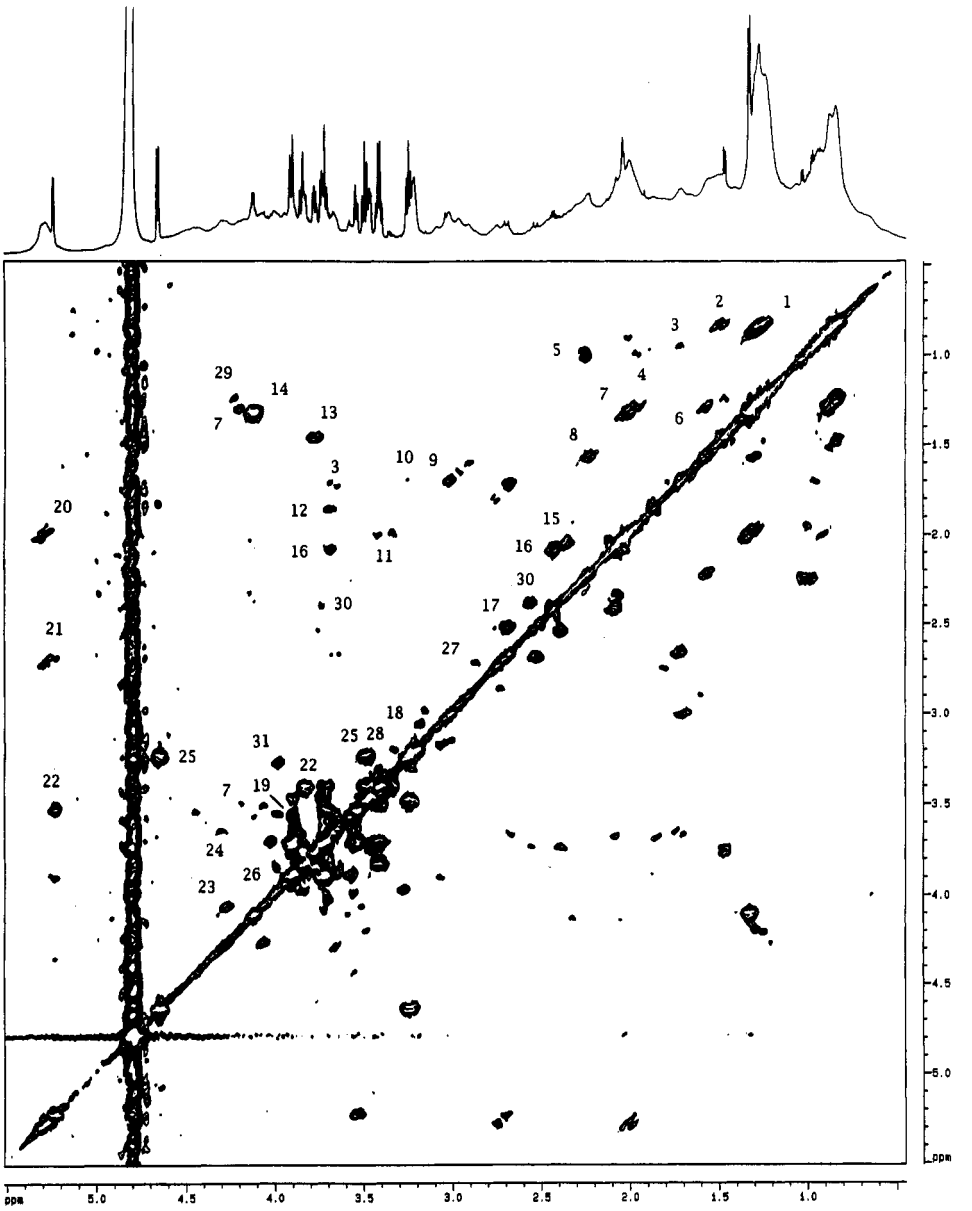

Figure 5. 750 MHz ^{1}H COSY 45 spectrum of control human plasma measured at 292 K (linear predicted in F1 and F2, not symmetrized), showing the region δ 0.45–5.50 with the one-dimensional spectrum of the same sample shown above. Key: FA, fatty acids of lipids; PC, phosphatidylcholine; TG, triglycerides; 1, CH_3CH_2 FA; 2, $CH_3CH_2CH_2CH_2$ FA; 3, leucine; 4, isoleucine; 5, valine; 6, $CH_2CH_2CH_2CO$ FA; 7, threonine; 8, CH_2CH_2CO FA; 9, lysine residues in albumin; 10, arginine; 11, proline; 12, citrulline; 13, alanine; 14, lactate; 15, glutamate; 16, glutamine; 17, citrate; 18, tyrosine; 19, glycerol; 20, CH_2CH= FA; 21, $CHCH_2CH$= FA; 22, α-glucose; 23, glycerol in PC/TG; 24, OCH_2CH_2N of PC; 25, β-glucose; 26, serine; 27, aspartate; 28, phenylalanine plus histidine; 29, fucose; 30, unknown 1; 31, unknown 2.

components that the two experiments observe. In particular, COSY spectra of plasma, like single pulse and ^{1}H–^{13}C HMQC spectra (see below), are dominated by signals from high M_r species, whereas CPMG and JRES spectra are dominated by signals from low M_r species. ^{1}H–^{1}H COSY spectra provide an additional assignment aid enabling the confirmation of the presence of a number of amino acid resonances including all those of valine, alanine, leucine, isoleucine, threonine, and glutamine and the majority of the resonances of others in diagnostic regions of the spectrum. These include the γCH_2–δCH_2 connectivity in lysine, the βCH_2–γCH_2 and γCH_2–δCH_2 of arginine, the αCH_2–βCH_2 and γCH_2–δCH_2 of proline, and the αCH–βCH_2s of citrulline, tyrosine, histidine, asparagine, and glutamate. A number of other small molecules can be observed in COSY spectra, including the acids 3-D-hydroxybutyrate, citrate, taurine, and lactate, as well as polyols such as *myo*-inositol and all resonances of α- and β-glucose.

The resolving power of the 750 MHz ^{1}H–^{1}H COSY experiment is also demonstrated by the connectivities observed for many of the resonances from the abundant plasma lipids which are not observable in the JRES experiment because of their short proton T_2 relaxation times (Figure 5). Thus connectivities for adjacent aliphatic protons, such as those in $CH_3CH_2CH_2CH_2CO$, CH_3CH_2-CH_2CH=, $CH_3CH_2(CH_2)_n$, and =$CHCH_2CH$= side chains of lipids, can be observed. The 750 MHz ^{1}H–^{1}H COSY spectrum provides excellent resolution in the olefinic proton chemical shift region. Here, apart from the resonance of the α-glucose anomeric proton, appear six cross-peaks which arise from olefinic protons in unsaturated lipids (see Table 1). Those at δ 5.23, 5.26, and 5.29 show connectivities to the proton chemical shifts at ca. δ 2.7 and

hence arise from olefinic protons adjacent to a CH_2 group between two double bonds, i.e., $CH{=}CHCH_2CH{=}CH$. It is not possible to resolve the olefinic proton spin−spin coupling and hence unambiguously determine whether the configuration is cis or trans. However, it is known that naturally occurring lipids are in the cis form. The three cross-peaks at δ 5.27, 5.31, and 5.33 show COSY connectivities to the ^1H chemical shifts near δ 2.0 and hence arise either from olefinic diene protons adjacent to CH_2 groups in an alkyl chain ($CH_2CH_2CH{=}CHCH_2CH{=}CHCH_2CH_2$) or from olefinic protons from a single isolated double bond in a lipid alkyl chain ($CH_2CH_2CH{=}CHCH_2CH_2$). ^{13}C chemical shifts from the HMQC spectrum (see below and in Table 1) also support these assignments.[41] The latter two situations can be distinguished by integration of the signals at δ 2.0, 2.7, and 5.3 in the one-dimensional spectra, which shows that for all of the plasma samples examined in this study, the olefinic proton signals come almost exclusively from lipids in the *cis*-1,4 diene arrangement rather than from isolated double bonds. Casu et al.[42] have previously used ^1H NMR spectroscopy to determine the relative levels of lipids in extracts of human blood plasma, and these data have compared favorably in terms of quantitation with more laborious HPLC analyses. From that work, it can be deduced, on the basis of known concentrations, that there are only three lipid classes which need to be considered in this assignment of COSY spectra of whole blood plasma: triacylglycerols, phosphatidylcholine, and sphingomyelin. In other recent studies involving the measurement of COSY spectra of choroform/methanol extracts of plasma, diagnostic cross-peaks were seen for the nonequivalent CH_2 group at C_1 of the glyceryl moiety of phosphatidylcholine and/or triacylglycerols. In addition, the cross-peak from the $OCH_2CH_2N^+$ group of phosphatidylcholine was observed, as were the cross-peaks for the connectivity between the methylene at C_1 and the methine protons at C_2 of the glyceryl moiety in lipids such as triglycerides or, more likely in view of its high concentration, phosphatidylcholine.[43] These signals were also seen in the 750 MHz COSY spectra of whole blood plasma, with a cross-peak at δ 4.06/4.24 corresponding to the geminal coupling for the C_1 methylene protons and a cross-peak at δ 3.67/4.30 corresponding to the coupling between the NCH_2 and OCH_2 groups of phosphatidylcholine.

There are also certain well-resolved signals observed in the 750 MHz COSY spectra of whole blood plasma which arise from domains of serum albumin (66 kDa) which have a relatively high level of molecular mobility, and some of these have been partially assigned.[44] Particularly strong are the cross-peaks from various lysine residues (δ 1.71/2.70, 1.79/2.74, and 1.59/2.90), which can also be detected in the $^1H-^{13}C$ HMQC spectra of blood plasma (see below). It is likely that these positively charged lysyl residues are on the outside of the protein and less motionally constrained than other amino acid residues, yielding relatively sharp lines. Peaks arising from two major three-spin systems are also observed, but these have not yet been assigned (U1 and U2). These have chemical shifts at δ 2.39/2.54/3.75 and 3.26/3.54/3.98. The former (U1) has shifts similar to those of aspartate and probably contains a similar CH_2CH fragment. The latter (U2) also contains a CH_2CH moiety, possibly of the type $CHOHCH_2OH$.

Two-Dimensional $^1H-^{13}C$ Heteronuclear Multiple Quantum Coherence Transfer Spectroscopy of Plasma, Albumin, and Lipoproteins. 750 MHz $^1H-^{13}C$ inverse-detected HMQC spectra of blood plasma have been measured and are reported here for the first time (Figure 6). This experiment provides strong peaks for the lipid resonances from HDL and LDL for a variety of small molecules and selected protein residues. $^1H-^{13}C$ HMQC spectra were recorded at 292 and 310 K, and the latter spectrum is shown in Figure 6. The upper traces in Figure 6 (A and B) correspond to the spectra processed with no time domain manipulation other than a shifted sine-bell-squared function prior to FT. The lower traces (C and D) result from processing the time domain data using the technique of linear prediction.[33] This process extends the limited digital resolution caused by the small number of increments in t_1 by computing values based upon extrapolation rather than by simple zero-filling of the FIDs. At both measurement temperatures, the $^1H-^{13}C$ HMQC spectra provided useful assignment data for the lipid resonances, enabling the distinction of all the major types of fragment. The cross-peak patterns obtained at 292 K were essentially similar to those obtained at 310 K, although the intensities of the signals from lipoproteins were stronger in the latter case, presumably owing to a general increase in the molecular mobility and lowering of the plasma viscosity. The use of linear prediction clearly improves the resolution within the cross-peaks in the ^{13}C chemical shift domain. A variety of signals of varying intensity were obtained in the HMQC spectra.

To aid assignment of the signals, 600 MHz $^1H-^{13}C$ HMQC spectra were obtained on human serum albumin, cholesterol linoleate, LDL, and α_1-acid glycoprotein (Figure 7). Many strong HMQC cross-peaks were obtained from all of these species, and the signals were extensively assigned. Several strong signals from mobile lysine residues (^1H δ 2.8−3.1 and ^{13}C δ 40.3 for various ϵ-CH_2s) for albumin and α_1-acid glycoprotein (much weaker) were observed, and collectively these gave rise to a very strong feature in the plasma HMQC spectrum (Figure 6). There were many other strong signals from the lipoproteins and cholesterol, and cholesteryl signals within these structures were assigned in plasma. The $^1H-^{13}C$ HMQC spectrum of LDL was particularly rich in information, with many methylene signals from fatty acid side chains in different environments being detected. The 750 MHz $^1H-^{13}C$ HMQC spectra of blood plasma lacked the individual detail shown in the spectra of the isolated proteins and lipoproteins. This would be expected because of the greater viscosity of plasma leading to shorter ^1H T_2 relaxation times. In the 750 MHz HMQC spectra, strong cross-peaks were observed for the C26/27 CH_3 groups of cholesteryl species, lactate, and alanine CH_3 signals, $N^+(CH_3)_3$ groups of choline-containing molecules, signals from the OCH_2 and NCH_2 groups of phosphatidylcholine, and all of the resonances of α- and β-glucose (Figure 7). The C18 axial CH_3 groups of cholesteryl species present in HDL particles were also detected in HMQC spectra and were stronger at 310 than at 292 K. This signal has also been assigned

(38) Bruyn, A.; Anteunis, M.; Garegg, P. J.; Nordberg, T. *Acta Chem. Scand. B* **1976**, *30*, 830−824.
(39) Bell, J. D.; Brown, J. C. C.; Kubal, G.; Sadler, P. J. *FEBS Lett.* **1988**, *235*, 81−86.
(40) Lentner, C., Ed. *Geigy Scientific Tables*; Ciba-Geigy: Basel, 1981; Vol. 1, pp 64−95.
(41) Gunstone, F. D.; Pollard, M. R.; Scrinmgeour, C. M.; Vedanayagam, H. S. *Chem. Phys. Lipids* **1978**, *18*, 115−129.
(42) Casu, M.; Lai, A.; Pilia, A.; Casti, G.; Zedda, S.; Gibbons, W. A. *Arch. Gerontol. Geriatr. Suppl.* **1992**, *3*, 111−122.
(43) Kriat, M.; Vion Drury, J.; Confort-Gouny, S.; Favre, R.; Viout, P.; Scoaky, M.; Sari, H.; Cozzonne, P. J. *J. Lipid Res.* **1993**, *34*, 1009−1019.
(44) Patel, S. V.; Sadler, P. J.; Tucker, A.; Viles, J. H. *J. Am. Chem. Soc.* **1993**, *115*, 9285−9286.

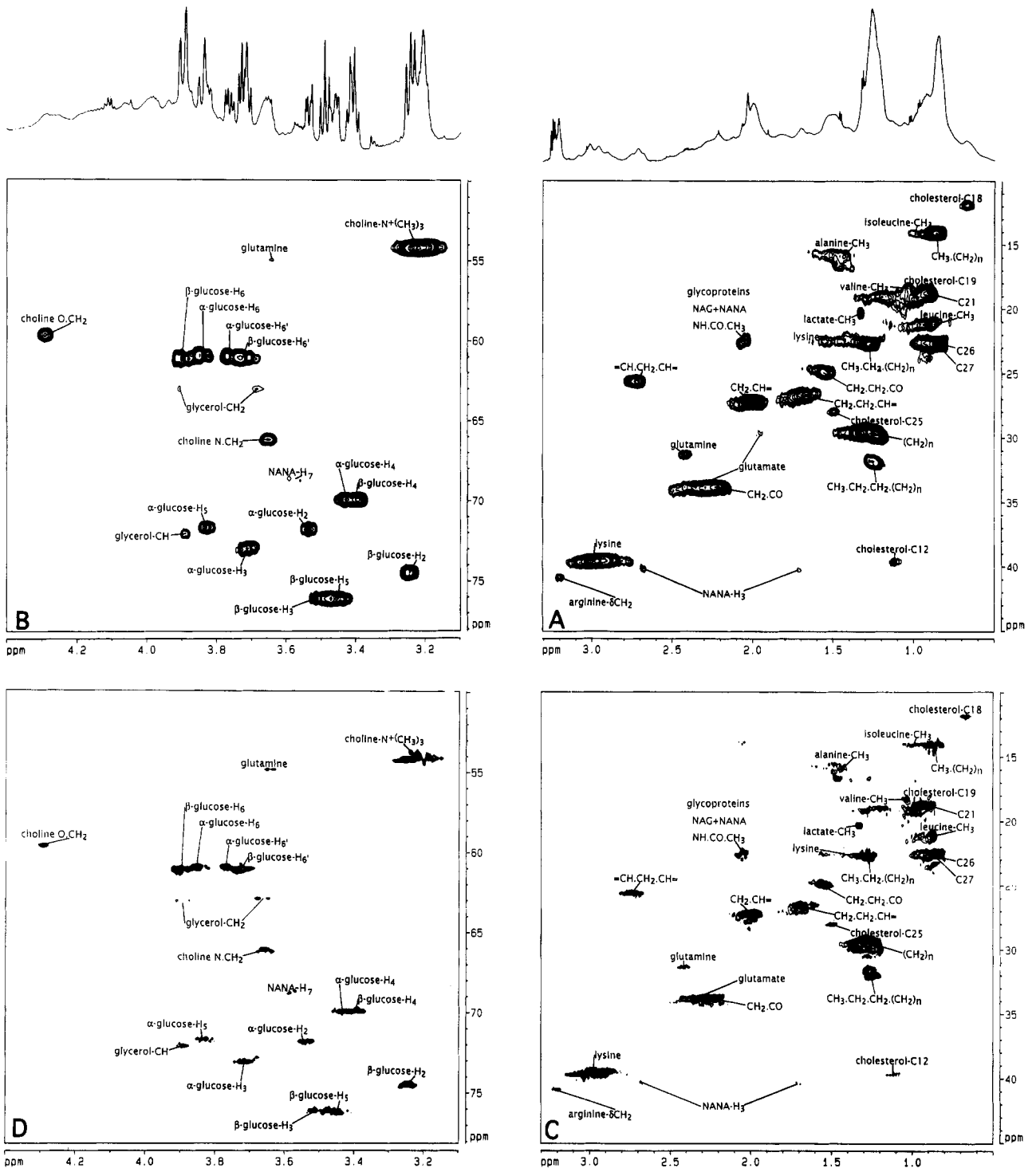

Figure 6. 750 MHz $^1H-^{13}C$ HMQC spectrum of control human plasma measured at 313 K, showing regions ^1H δ 0.5–3.3, ^{13}C δ 10–50 (A and C) and ^1H δ 3.1–4.4, ^{13}C δ 50–80 (B and D). The corresponding regions of the 1-D 750 MHz ^1H NMR spectum collected on the same sample are shown above spectra A and B. The spectra shown in (A) and (B) were processed with shifted sine-bell-squared time domain functions in both F1 and F2, and (C) and (D) demonstrate the use of forward complex linear prediction of the data points in the F1 dimension, as described in the Experimental Section. Assignments are as labeled and as given in Table 1.

assigned by others using ^1H NMR methods.[13] The resonances of free glycerol are observed, with the C_1 and C_3 methylene groups having ^1H shifts of δ 3.56/3.64 and a ^{13}C shift of δ 63.5 and with the C_2H methine having a ^1H shift of δ 3.87 and a ^{13}C shift of δ 72.6. In addition, the cross-peaks corresponding to glyceryl CH_2 moieties in lipids such as triglycerides and phosphatidylcholine are observed, with proton shifts δ 4.04 and 4.25 and ^{13}C shifts of δ 62.0 (these signals are not depicted in the figures but can be seen at lower contour levels); the glyceryl CH was too weak to be observed. The signals for all lipid moieties were much more intense in the HMQC spectra measured at 310 K relative to those of the low M_r metabolites. Cholesterol CH_3 signals were 3–4 times as intense in $^1H-^{13}C$ HMQC spectra at 310 K as they were at 292 K, consistent with the greater motional freedom of the lipoprotein particles (see below).

Effects of Temperature Variation on the 750 MHz NMR Spectra of Blood Plasma. The 1-D 750 MHz ^1H spectra of a control blood plasma sample measured at 292 and 310 K are

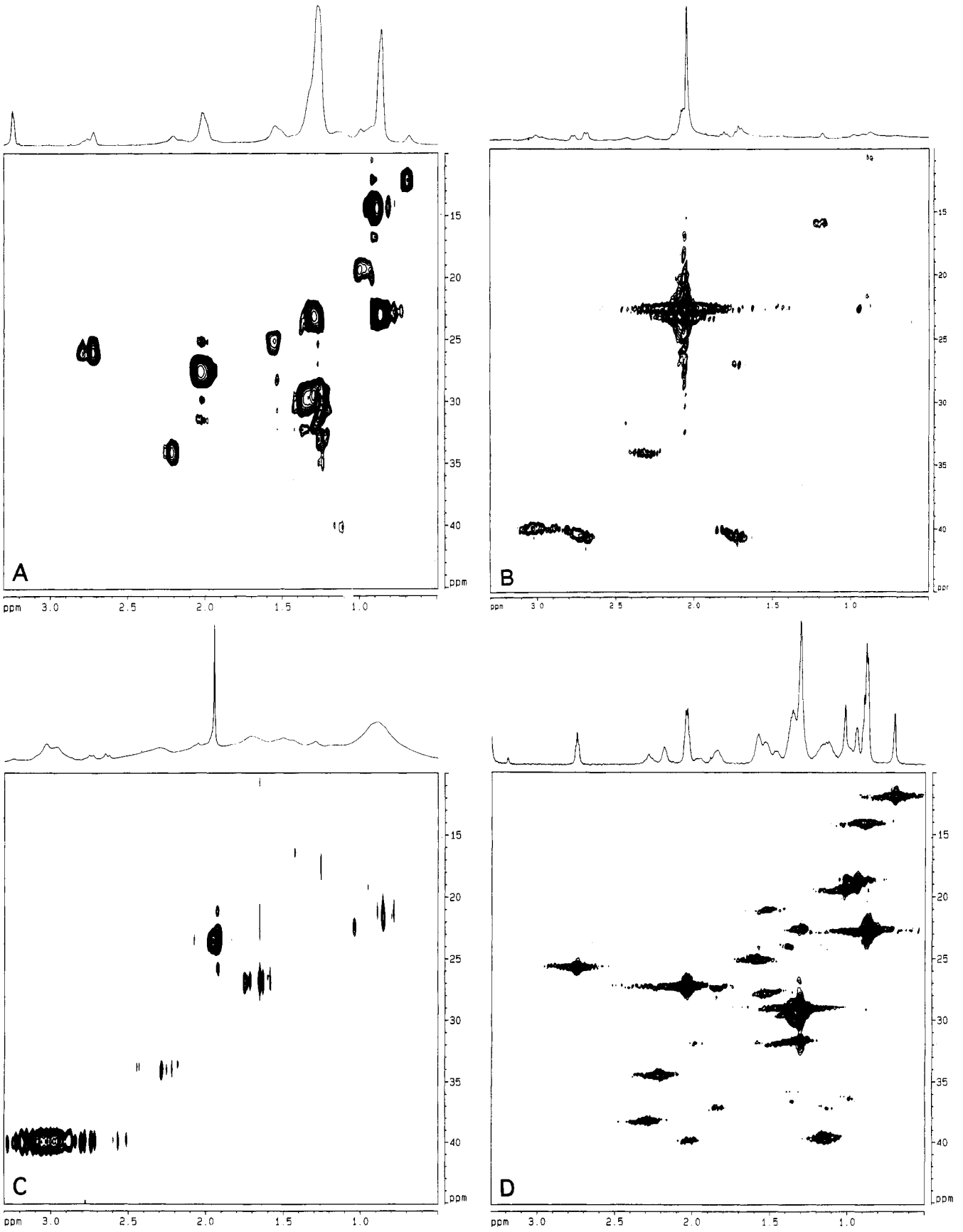

Figure 7. 600 MHz $^{1}H-^{13}C$ HMQC spectra measured at 310 K (same regions as Figure 6A) of major plasma components. (A) Low-density lipoprotein; (B) α_1-acid glycoprotein; (C) human serum albumin, all in aqueous solution; and (D) cholesterol linoleate in $D_2O/CD_3OD/DMSO$-d_6 (1:2:1). All spectra were linear predicted in F1 and F2.

shown in Figure 8A and B, respectively. On increasing the temperature, all of the lipid resonances increase in intensity relative to the resonances of the small molecules which remain constant. The increase in intensity is accompanied by a significant

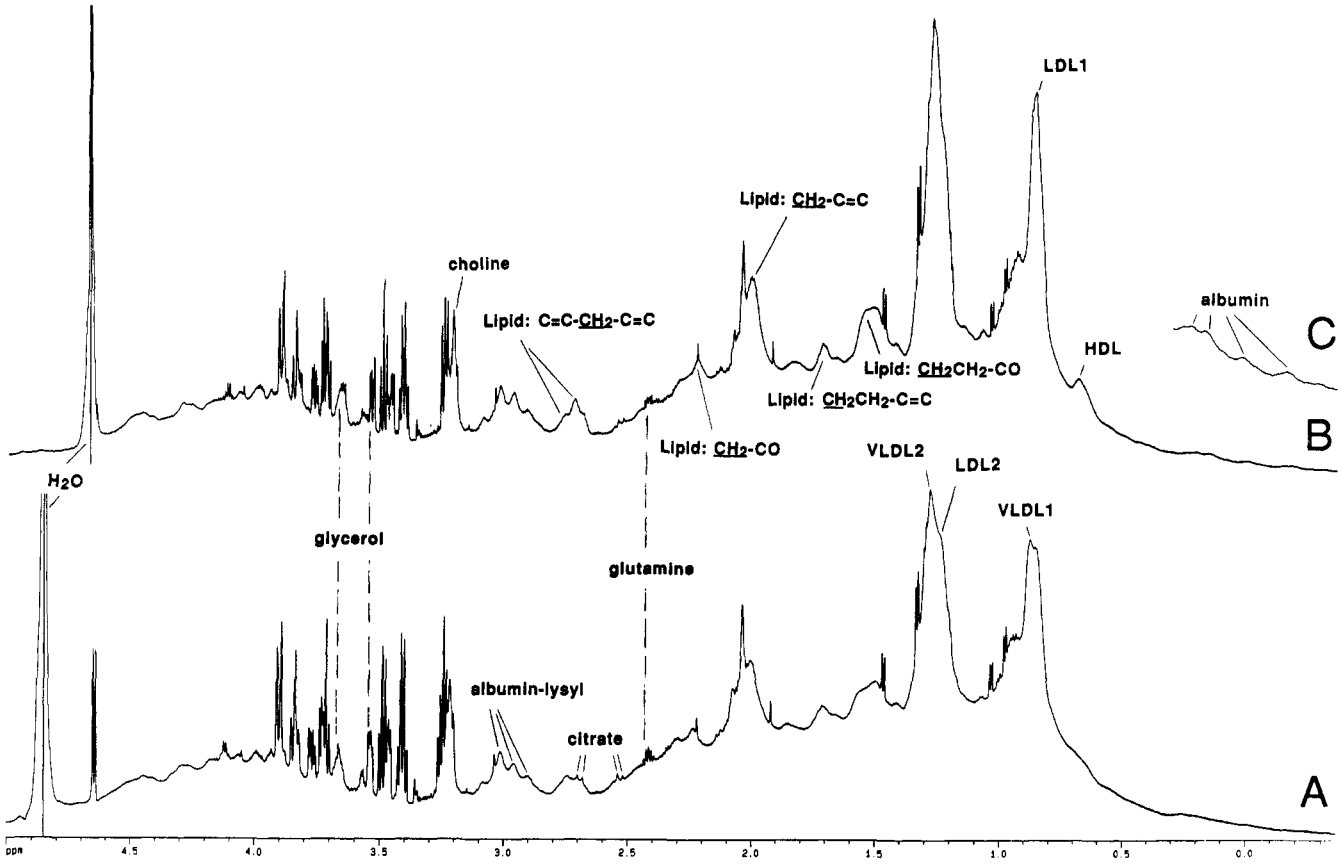

Figure 8. Effect of changing the temperature on the single pulse 750 MHz ^{1}H NMR spectra of control human blood plasma (δ −0.4 to 5.0) (A) at 292 K, (B) at 310 K, and (C) at 310 K with 4× vertical expansion of the spectrum. Assignments are as labeled or as given in Figure 1.

sharpening of the resonances. This implies, therefore, that the lipoprotein line widths are dominated by T_2 relaxation rather than a dispersion of chemical shifts, and from the inverse relationship between T_2 and the rotational correlation time, as the particles become more motionally mobile at the higher temperatures, as expected, the T_2 values are increased. With increasing temperature, the lipid CH_3 and CH_2 signals appear to sharpen and increase in intensity consistent with the increases in intensity of the ^{1}H−^{13}C HMQC cross-peak when measured at the higher temperature (Figure 6). Selective changes are also visible, e.g., the cholesteryl C18 axial CH_3 group of HDL progressively sharpens and increases in intensity (intermediate 298 and 304 K steps not shown), as do the signals from some of the ring current-shifted CH_3 groups of amino acids in albumin (Figure 8C). These HDL and albumin signals are not normally resolved in NMR spectra measured at lower frequencies and have not been identified in previously published NMR work on whole blood plasma. Other lipid resonances also increase in intensity with temperature, particularly those from the CH_2 protons at δ 1.2, the CH_2CH=CH signal at δ 2.0, the HC=CHCH_2CH=CH signal at δ 2.7 (which completely obscures the high frequency citrate signals at 310 K), the choline $N^+(CH_3)_3$ signal at δ 3.25, and the CH=CH signal at δ 5.1 (not shown). Two partially resolved signals from glycerol also sharpen with increasing temperature and the spin−spin coupling pattern for the γ-CH_2 of glutamine also changes, probably indicating a slight change in conformation of the molecule or of the nonequivalence of the methylene ^{1}H chemical shifts. As would be expected, the plasma water signal also shifts to low frequency with increasing temperature, hence obscuring the H_1 anomeric proton signal of β-glucose.

Further information on the selective effects of temperature on the molecular mobility of substances dissolved in blood plasma can be gained by inspection of the 750 MHz ^{1}H CPMG spin−echo spectra measured at 292, 298, 304, and 310 K in the range δ 0.7−5.5, as shown in Figure 9 for the aliphatic region of the spectrum. Interpretation of intensity changes with temperature in CPMG spectra must be treated with caution. For small molecules with short rotational correlation times (τ_c), the proton T_1 values (which are dominated by dipolar relaxation) will be equal to T_2. Increasing the temperature will shorten τ_c and lengthen the T_1 and T_2 values, with a consequent reduced signal attenuation in CPMG spin−echo spectra without any sharpening of the lines. If the T_2 values are long compared to the interpulse delays, there will be minimal changes. On the other hand, macromolecules have τ_c values outside the motional narrowing limit, i.e., where $\omega^2\tau_c^2 \gg 1$, and in this case, $T_1 \neq T_2$. Increasing the temperature will again shorten τ_c, in this case leading to a shorter T_1 but a longer T_2. Thus, resonance intensities in the CPMG spectra will be decreased if T_1 relaxation occurs in the interpulse delays and will increase because of the lengthened T_2 values. In addition, the T_2 values are likely to be short enough to cause line-broadening effects, and any lengthening of the T_2 values by increasing the temperature will result in line-sharpening. The signals from the low M_r species such as lactate, acetate, alanine, and valine did not increase in intensity with increasing temperature. Previous reports indicated that a significant proportion of plasma lactate is bound to α_1-acid glycoprotein and transferrin and that these bound forms can be released by addition of detergents.[38] However, the lactate signal intensity or line width appeared virtually unchanged from 292 to 310 K. This indicates

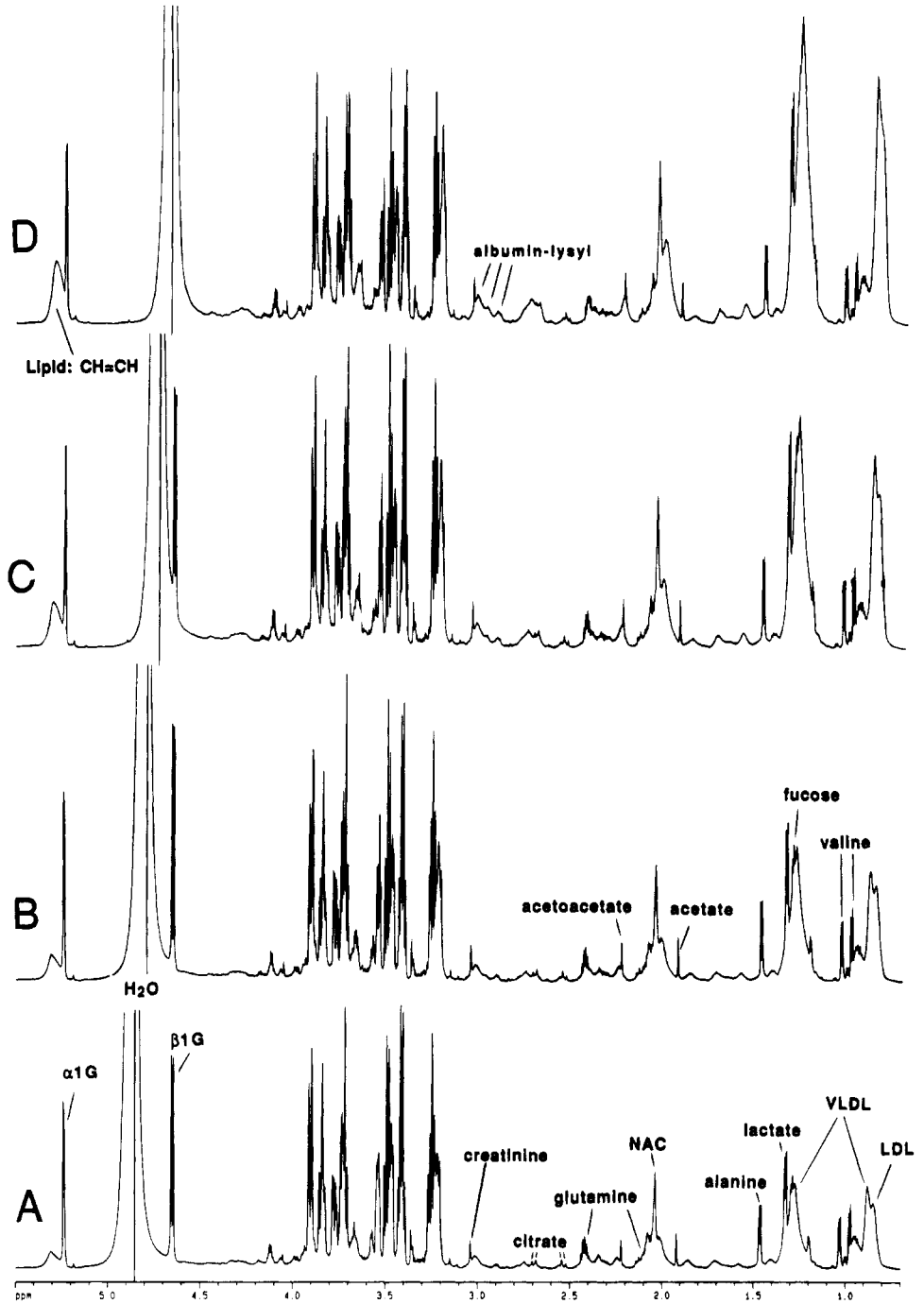

Figure 9. Effect of changing the temperature on the 750 MHz CPMG ^{1}H NMR spectra of normal human blood plasma (δ 0.4–5.0) (A) at 292 K, (B) at 298 K, (C) at 304 K, and (D) at 310 K. Assignments are as labeled or as given in Table 1.

that the access of lactate from any protein-bound compartment to free solution was not altered or that there is a significant excess of free over bound lactate with the proportions of the two not changing greatly over this temperature range.

All lipoprotein signals increased in intensity in CPMG spectra with increased temperature; thus, spin–echo spectral editing to remove signal from short T_2 components will be more efficient at lower temperatures, as the signals from albumin and lipoproteins are significantly broader. In effect, this means that a shorter $2n\tau$ period in the spin–echo pulse sequence is required to attenuate the macromolecular signals with less distortion of signal intensities of the low M_r metabolites. The intensity of the LDL and VLDL CH_3 signals did not increase markedly from 292 to 298 K, but did increase from 298 to 310 K. The LDL CH_3 signals also increased in intensity relative to the VLDL CH_3 signals with increasing temperature, and LDL dominates the low-frequency lipoprotein CH_3 signal complex at 310 K. This is consistent with the known selective temperature dependence of the LDL signal line widths in purified lipoprotein samples.[16] VLDL particles cover the size range 300–800 nm, whereas LDL particles are in the 190–290 nm range,[45] but the reported half-height line widths of the VLDL CH_3 and CH_2 groups are less than those of the LDL, indicating greater internal mobility in the larger particles.[16] This implies, not surprisingly, that the line widths are dominated by internal molecular motions rather than the bulk motional properties of the particles. The disproportionate increase in the T_2 relaxation

(45) Dawson R. M. C.; Elliot, D. C.; Elliot, W. H.; Jones, K. M. *Data For Biochemical Research*; Clarendon Press: Oxford, 1990; p 404.

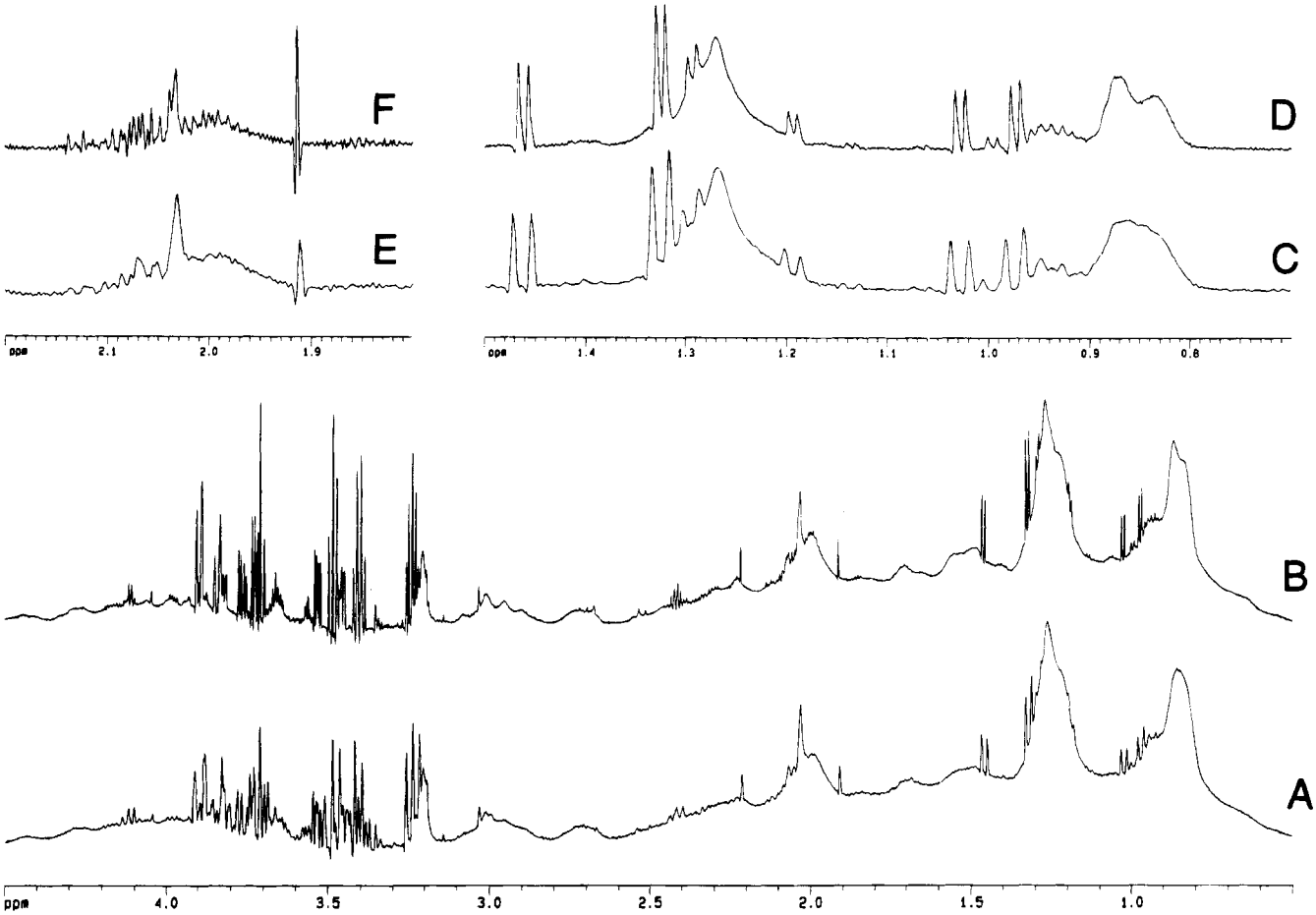

Figure 10. Effect of ^1H observation frequency on the 1-D NMR spectrum of control human blood plasma. (A) 400 MHz 1-D spectrum (δ 0.5–4.5); (B) 750 MHz 1-D NMR spectrum (δ 0.5–4.5); (C) 400 MHz CPMG spectrum (δ 0.7–1.5); (D) 750 MHz CPMG spectrum (δ 0.7–1.5); (E) as spectrum C but δ 1.8–2.2; and (F) as spectrum D but δ 1.8–2.2.

time of the LDL CH_3 and CH_2 signals over those of VLDL with increasing temperature means that the segmental motion of the LDL aliphatic lipid chains must also increase more than in VLDL. The present observations appear to confirm that this extra temperature-dependent mobility of LDL is maintained in intact blood plasma and is not an artifact of purification.

The aromatic proton region of the 750 MHz CPMG ^1H spin–echo spectrum from δ 6.4 to 8.6 contains relatively few signals (data not shown). The signal intensities for formate and histidine appear to be unaffected in the temperature range 292–310 K, but signals from tyrosine and phenylalanine are substantially increased in intensity at 304 and 310 K (relative to formate and histidine) but were not shifted. Previous studies have shown that both phenylalanine and tyrosine are extensively bound by plasma proteins, so their signals are not visible in 400 MHz Hahn spin–echo ^1H NMR spectra (using $2n\tau$ = 136 ms) of normal human plasma at neutral pH and when measured at 292 K, but that signals from these amino acids were increased in Hahn spin–echo spectra at low pH. Two broad singlets at δ 7.50 and 6.95, assigned to the CH signals of 3-methylhistidine, appear to show a temperature-dependent behavior similar to that of tyrosine.

Frequency Dependence of ^1H NMR Spectra of Blood Plasma. With increasing observation frequency, there are marked improvements in the overall information content of the ^1H NMR spectra of blood plasma at the same temperature, 292 K. This is illustrated by comparing the 400 and 750 MHz spectra of plasma, all plotted at the same line width in hertz and on the same chemical shift scale, i.e., simple one-dimensional spectra (Figure 10A and B), the resolution-enhanced CPMG spin–echo spectra of the CH_3 region (Figure 10C and D), and the resolution-enhanced CPMG spectra of the acetyl region (Figure 10E and F). There is still extensive signal overlap in all regions of the ^1H NMR spectrum, even at 750 MHz. However, the improved dispersion at 750 MHz allows separate signals from the VLDL and LDL terminal CH_3 groups to be resolved (Figure 10C and D), which is important given the potential clinical significance of these measurements and the necessity of performing extensive line shape analysis and deconvolution for their quantitative measurement in NMR spectra.[16] The CH_3 doublet signals of 3-D-hydroxybutyrate and fucose are both better resolved on either side of the lipoprotein CH_2 signals, and the CH_3 doublets of valine, leucine, and isoleucine are dispersed, allowing the identification of the latter. The CH_3 doublet of isoleucine can only be fully resolved from the CH_3 doublets of valine at 750 MHz. At 750 MHz, the broad lipid signal at δ 2.01 is partly resolved from the major α_1-acid glycoprotein signal at δ 2.03 but remains much more extensively overlapped at 400 MHz (Figure 10E and F), and as shown earlier, other low M_r metabolite signals may also occur in this region (Figures 2 and 3). This indicates that there may be potential problems with using the *N*-acetyl signal for diagnostic purposes when it has been measured at lower frequencies, as has been suggested by some other workers.[35,36] Resolved signals from the three major lysyl ϵ-CH_2 signals from mobile regions of albumin can be partially resolved at 750 MHz but are unresolved at 400

MHz (Figure 10A and B). All four citrate resonance lines are clearly visible at 750 MHz but are heavily overlapped with residual lipid signals at 400 MHz. The choline $^{+}N(CH_3)_3$ signal is also separated from the H_2 signal of β-glucose at 750 MHz (Figure 10B). At 750 MHz, the creatinine signal is better, though still incompletely, separated from a composite peak (which includes the lysyl ϵ-CH_2 signal) at δ 3.05 (Figure 10B). The H_1 anomeric proton signal of β-glucose is also much better separated from the water signal at 750 MHz and is nearly baseline resolved (data not shown). Solvent suppression is also more selective at 750 MHz because of the increased frequency separation from other signals and results in more effective attenuation of the water signal by about a factor of 3 compared with optimized 400 MHz measurements. There is improved separation of the broad lipid olefinic proton signals at δ 5.27 from the H_1 anomeric proton signal of α-glucose at δ 5.233, although resolution is still incomplete (Figure 8A) . The remaining complex of signals from α- and β-glucose have much less second-order character at 750 MHz than at 400 MHz and hence can be interpreted much more easily. Similarly, signals from glycerol can also be identified in 750 MHz single pulse spectra but are heavily overlapped with glucose signals and have much greater second-order character at 400 MHz (Figure 10A and B).

Biochemical Information in High-Frequency ^{1}H NMR Spectra of Blood Plasma. The biochemical information content of ^{1}H NMR spectra of blood plasma (and other biofluids) is high in terms of both the number of detectable metabolites and the types of observable dynamic molecular interactions.[1] Even a cursory examination of the 750 MHz NMR spectra shown in Figures 1–5 reveals that there is always an advantage of working at the highest possible observation frequency when making measurements on blood plasma. Apart from improvements in sensitivity and dispersion, there is also a general translation of the level of information available. For resonances which are well separated from each other, for example in the olefinic region of the spectrum (δ 5.5–6.5), increasing the observation frequency results directly in a lower detection limit. This is because the noise in the spectrum in this region is dominated by electronic spectrometer noise. The usual arguments relating to the increased sensitivity at higher frequency will be sure to apply. However, in other regions of a biofluid spectrum where peaks are much more crowded, the benefits of increased sensitivity and dispersion at higher operating frequencies are closely interrelated. In this situation, the true spectral noise is generally hidden in the spectrum by a multitude of small overlapping NMR resonances, which has been termed "chemical noise".[1]

Chemical noise is the result of the extensive overlap of signals from many compounds at low concentrations in biofluids and close to the detection limit of the NMR spectrometer (ca. 1–10 μM), but collectively these give rise to apparently broad and featureless NMR signals because their line widths are greater than the separation of any two components. Increasing the digital resolution of the experiment has no effect in this case, and it is the chemical noise rather than electronic noise that is the factor which is limiting the spectral information content. By definition, no single component of the chemical noise envelope can be resolved or useful information extracted irrespective of the NMR experiment performed. In order to probe a range of biochemical processes, it may be necessary to detect metabolites over a wide concentration range. Even with water suppression, it is easy to visualize a situation where a metabolite has a concentration of 100 nM in a fluid where another metabolite is present at 5 mM, e.g., glucose in blood plasma. This represents a dynamic range of approximately 17 bits, and this may limit the digitization of signals from low-abundance metabolites. Other biofluids such as urine may contain 20–30 mM creatinine and 0.5 M urea, and again dynamic range limitations may apply if there is a need to detect low-level components.[1]

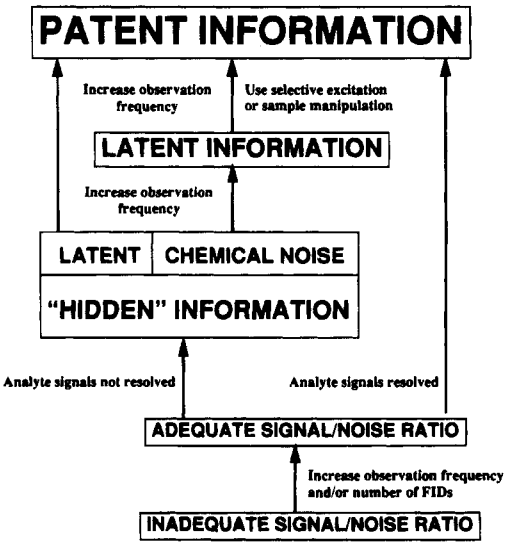

Figure 11. Schematic diagram illustrating the possible relationships between the ^{1}H NMR spectral information content of biofluids and observation frequency.

There are two types of accessible biochemical information available from an NMR experiment on a biological fluid: these can be termed *patent* and *latent*. We define patent information as arising from metabolite signals that are sufficiently resolved and intense to be measured quantitatively in the 1-D experiment at a particular NMR frequency. The latent information in an NMR spectrum measured at a particular field as defined here is *not* available in the 1-D spectrum; thus useful biochemical data can only be obtained by careful selection of an appropriate multipulse sequence to achieve either spectral editing or frequency dispersion in a second or higher dimension. Increasing the observation frequency and hence dispersive power of a spectrometer leads directly to less overlap of the chemically shifted resonances observable. This can clearly improve the information content by converting some of the latent data to patent data. In addition, the species which had contributed to the chemical noise envelope may now be partly resolvable and this may give rise to latent information. On increasing the NMR frequency, there are always translations from chemical noise to latent information and from latent to patent information in biofluid spectra. The logic of this argument is encapsulated in Figure 11.

Biochemical information can be latent in NMR spectra through multiple resonance overlap and/or dynamic molecular interactions with other species, in both cases resulting in a lack of resolved signals for compounds present in plasma at levels well within the normal NMR detection range, e.g., cholesterol and its esters, which are constituents of lipoproteins in blood plasma that are present at millimolar levels but are not normally detectable in 1-D spectra.[6] In the case of latency, the use of multidimensional NMR

(46) Spraul, M.; Nicholson, J. K.; Lynch, M. J.; Lindon, J. C. *J. Pharm. Biomed. Anal.* **1994**, *12*, 613–618.

can lead to a conversion to patency. Alternatively, if some resonances of a given molecule are patent, then selective excitation techniques, e.g., 1-D TOCSY, may be useful.[46] In addition, the use of spectral deconvolution such as maximum entropy processing[47-49] can give a substantial line-narrowing, thereby minimizing the problem. In the case of latency due to dynamic interactions, data may be made patent either by changing observation frequency, for instance, in the case of some chemically exchanging species, or by altering the NMR measurement conditions,[40] e.g., temperature (Figure 7) or pH, to increase the molecular mobility of tyrosine and phenylalanine, which can bind to plasma proteins, or to ensure that the cholesteryl esters are above their liquid crystal isotropic transition temperatures. Below this temperature, such molecules give broad and virtually undetectable resonances, but above the transition they give sharp liquidlike signals.

There has been and is likely to be much more debate about the "cost-effectiveness" of using very-high-frequency NMR spectrometers for biological fluid measurements. At lower measurement frequencies (250–400 MHz), although there is much patent information in the ^{1}H NMR spectrum, i.e., there are many metabolites that can be detected and quantified with some degree of accuracy and precision,[6] there are many more identifiable organic species detectable at higher frequencies. This additional spectral information allows a more effective exploration of the biochemistry of the system under study, and the precision and reliability of the metabolite measurements also improve because of the better spectrometer sensitivity. On the other hand, the increased sensitivity and dispersion at higher frequencies bring additional complexity to the ^{1}H NMR spectra, thus providing a greater assignment challenge. It is clear that at even the present level of technology in NMR, it is not yet possible to detect many important biochemicals, e.g., hormones, in body fluids because of problems with sensitivity, dispersion, and dynamic range, and this area of research will continue to be technology-limited. With this in mind, it would seem prudent to interpret quantitative ^{1}H NMR measurements of plasma and other biological fluids, in particular the clinical interpretation of such spectra, with considerable caution even when measurements are made at the highest NMR frequency available.

(47) Sibisi, S.; Skilling, J.; Brereton, R. G.; Laue, E. D.; Staunton, J. *Nature (London)* **1984**, *311*, 416.
(48) Laue, E. D.; Skilling, J.; Staunton, J.; Sibisi, S.; Brereton, R. G. *J. Magn. Reson.* **1985**, *62*, 437–452.
(49) Seddon, M. J.; Spraul, M.; Wilson, I. D.; Nicholson, J. K.; Lindon, J. C. *J. Pharm. Biomed. Anal.* **1994**, *12*, 419–424.

ACKNOWLEDGMENT

We thank the St. Peter's Trust for Kidney Research for supporting this and related projects and Professor G. H. Neild for valuable advice.

Received for review October 17, 1994. Accepted December 6, 1994.[⊗]

AC9410124

[⊗] Abstract published in *Advance ACS Abstracts,* January 15, 1995.